Industry Canada CRC

OPTO-ELECTRONIC TECHNOLOGY FOR THE OPTICAL CONTROL OF ARRAY ANTENNAS

by

Claude Bélisle

CRC TECHNICAL NOTE 93-003

September 1993
Ottawa

Industry Canada Industrie Canada

The work described in this document was sponsored by the Department of National Defence under Task 041LL.

Canada

OPTO-ELECTRONIC TECHNOLOGY FOR THE OPTICAL CONTROL OF ARRAY ANTENNAS

by

Claude Bélisle
DGSAT/MILSATCOM
Communications Research Centre, Ottawa

The work described in this document was sponsored by the Department of National Defence under Task 1410-0417W.

COMMUNICATION RESEARCH CENTRE, INDUSTRY CANADA
CRC REPORT NO. 93-003

Canada

September 1993
Ottawa

TABLE OF CONTENT

LIST OF ABBREVIATIONS

A	Ampere
A-O	Acousto-optics
APD	Avalanche photodiode
BFN	Beam forming network
dB	Decibel
CW	Continuous wave
DC	Direct current
E-O	Electro-optics
FET	Field effect transistor
FM	Frequency modulation
GHz	Gigahertz
GRIN	Graded Index
HEMT	High electron mobility transistor
IF	Intermediate frequency
kHz	Kilohertz
LCLV	Liquid crystal light valve
LED	Light emitting diode
LO	Local oscillator
mA	milliampere
MBA	Multiple beam antenna
MHz	Megahertz
MMIC	Microwave monolithic integrated circuit
MQW	Multiple quantum well
mW	Milliwatt
M-Z	Mach-Zhender
NA	Numerical aperture
PA	Phased array
PIN	Positive Intrinsic Negative
RF	Radio frequency
SLM	Spatial light modulator
SOA	Semi-conductor optical amplifier
TW	Travelling wave
W	Watt

ABSTRACT

In this report, concepts, components, performance analysis, system designs for an opto-electronic implementation of phased array and multiple beam antennas are reviewed. The aim of the report is to provide the reader with a basic understanding of what needs to be accomplished and an overview of the state of the art in opto-electronics components and systems.

RÉSUMÉ

Dans ce rapport, différents concepts, composantes, analyses de performance, et architectures de systemes pour la fabrication d'une antenne à ouverture de phase contrôlée opto-électroniquement sont revus. Le but du rapport est d'offrir au lecteur une compréhension sommaire de ce qui doit être accompli ainsi qu'un aperçu de l'état de la technologie au niveau des composantes électro-optique et des systèmes.

EXECUTIVE SUMMARY

Millimetre-wave active phased array antennas are becoming increasingly important for a number of applications where small and lightweight antennas are required such as for mobile ground, airborne, and spacecraft customers. Dynamically addressable beam steering and beam nulling capabilities are also particularly interesting from a military point of view. However, the large number of transmit/receive modules forming these antennas presents some demanding requirements not found in conventional antennas. Significant research is being done in the field of GaAs MMIC to provide a solution to the electronic radiative elements of the antenna, but the signal distribution to and from each of these elements creates formidable topology, EMI, and crosstalk problems. The phase and amplitude control of the different element signals, required to draw maximum profit from the beam steering and beam nulling capabilities of PA antennas, is also not a trivial matter.

Opto-electronic technologies are being proposed as an alternative for some of the tasks. For example, fiber optics could replace the conventional waveguides or coaxial cables for signal distribution. This would not only reduce considerably the weight and size of the system, but would also allow lower losses in the signal distribution, provide better interference immunity, and give higher bandwidth. Also, some of the signal processing tasks could take advantage of the parallel processing capabilities of optical systems. Two dimensional Fourier transforms and covariance matrix calculations, all required to compute the necessary phase and amplitude weighting, could be executed in real time with optics. Interconnections between the processing unit and the distribution system would also be made easier if both units were using optics.

In this paper, concepts, components, performance analysis, system designs are reviewed with the scope of integrating electronic and optical technologies to provide a viable alternative to the conventional microwave antenna design approach.

The conversion from the RF signal to the optical signal is analyzed. Three main techniques are presented (direct modulation, external modulator and heterodyne techniques). The best technique to use is application dependent, based on the RF frequency, power level, system integration requirements. Heterodyne techniques present a number of advantages over the other two modulation schemes but are the least mature.

The conversion back from optics to the electrical domain is also considered. Various techniques are also reviewed. Photodetectors are compared with conventional microwave components used as photodetectors. System integration possibilities is reviewed.

The theory behind beam forming network for array antennas is also reviewed. Various system considerations such as phase and amplitude resolution, frequency bandwidth, and time delays are reviewed to provide guidance in the selection of a beam forming network architecture. Generic as well as some specific architectures are proposed as a baseline for the development of more sophisticated, better performing ones for specific applications.

Finally the signal distribution function is approached. The different components of the network, such as, splitters, optical amplifiers, coupling, are reviewed and typical performances are given. A link budget example is also given for the transmit link of a proposed 1000 element antenna.

In conclusion, based on today's state of the technology, it is believed that opto-electronic can play a significant role in the design and fabrication of spaceborne array antennas. However, research is still needed both at the component and system levels.

1.0 INTRODUCTION

1.1 Background

Array antennas have the ability to rapidly beam steer with high gain and beam null for protection against interference. These features make them extremely attractive for a number of applications, both military and civilian. Mobile, airborne and spacecraft communications, where small and light weight antennas are required, may find a solution in phased arrays. Since beam steering is done electronically, no moving parts are needed; a definite advantage in radar systems.

The large number of transmit/receive elements forming these antennas (up to one hundred thousand for certain radar applications) presents some demanding requirements not found in conventional antennas. The signal distribution to and from each of these elements creates formidable topology, EMI, and crosstalk problems. The size and weight of the distribution network, when designed with conventional waveguides or coaxial cables, often become too big to be practical. Extremely demanding signal processing requirements are also needed to process information for hundreds or even higher numbers of elements. The phase and amplitude control of the different signals, required to draw maximum profit from the beam steering and beam nulling capabilities of PA antennas, is also not a trivial matter.

Opto-electronic technologies are being proposed as an alternative for some of the tasks. For example, fiber optics could replace the conventional waveguides or coaxial cables for signal distribution. This replacement would not only reduce considerably the weight and size of the system but would also allow lower losses in the signal distribution, better interference immunity, and higher bandwidth. Also, some of the signal processing tasks could take advantage of the parallel processing capabilities of optical systems. For example, two-dimensional Fourier transforms and covariance matrix calculations, used to compute the necessary phase and amplitude weighting, could be executed in real time with optics. Interconnections between the processing unit and the distribution system would also be made easier if both units were using optics.

1.2 Purpose

The scope of this report is to give an overview of the optical technologies which could find an application in the implementation of a phased array and multiple beam aperture. Concepts, components, performance analysis, system designs are also reviewed.

1.3 System definition

Phased array (PA) antennas essentially consist of a number of elements (some may have hundreds of thousands of elements) each radiating or receiving an RF signal. Fig. 1.1 gives a schematic representation of a PA. These antennas operate on the principle of interference between the signals emitted from the many discrete elements forming the antenna. These signals will add or subtract in amplitude at some point in space according to the phase and amplitude distribution at the antenna aperture. If all signals are of equal amplitude and phase, a beam will form in the direction normal to the antenna. However, if the phase and amplitude distribution changes, the interference pattern, and consequently, the beam profile will be modified. The transmitted beam may thus be steered in any direction or even be composed of a number of narrow beams by carefully adjusting the phase and amplitude of each element, and this, without having to physically move the antenna or any of its elements. Fig. 1.2 gives a schematic representation of a linear array. A variable phase shifter and an attenuator are associated to each element radiator to provide the proper phase and amplitude weight.

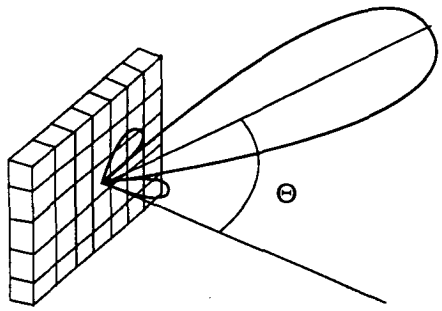

Figure 1.1 Schematic representation of a PA. The beam propagation angle depends on the phase and amplitude relation between the antenna elements.

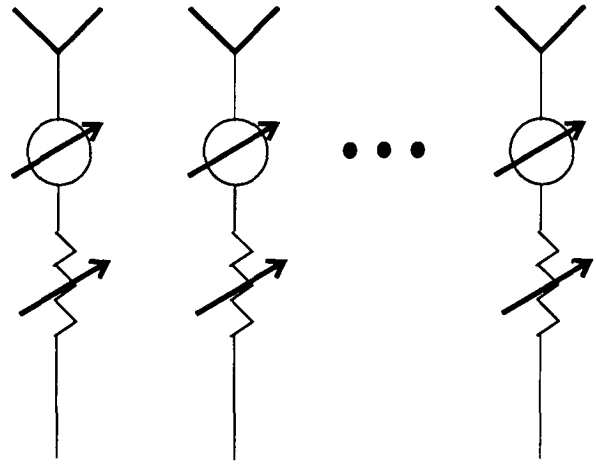

Figure 1.2 Schematic representation of a linear array. An attenuator and a phase shifter are associated to every element to provide the appropriate phase and amplitude.

Multiple-beam antennas (MBA), on the other hand, employ the more conventional horn/reflector team. In this case however, many horns are associated to the same reflector. Fig. 1.3 shows a schematic view of an MBA. The direction of propagation of the emitted beam is a function of the selected antenna horn. To each horn is associated a specific direction of propagation. In Fig. 1.4, a 3-horn MBA is schematically shown with the associated emitted beam from one element. Fig. 1.5 shows a map of Canada, with a possible spot beam configuration from a 31-horn MBA. Typically, MBA horns are clustered in groups of 3,7,9 or 19. A 3-beam and 7-beam clusters are shown in Fig. 1.6.

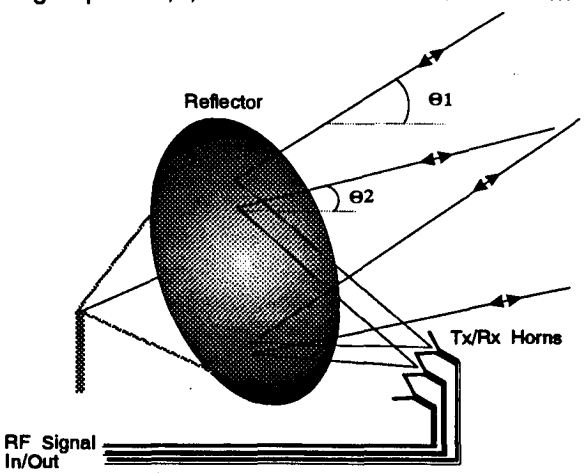

Figure 1.3 Schematic view of a multiple-beam antenna. To each horn is associated a specific beam.

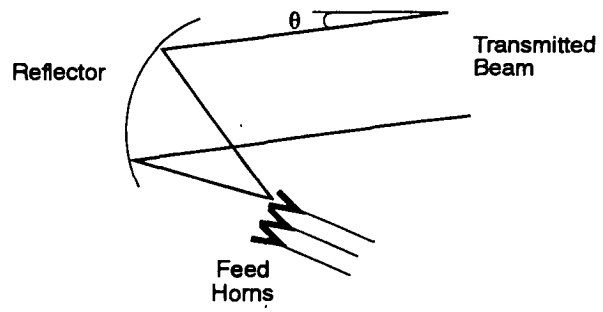

Figure 1.4 Schematic representation of an MBA with the 3 horns at the focal plane of the parabolic reflector.

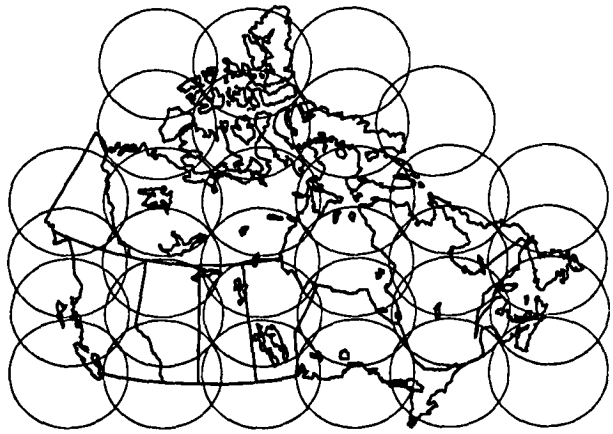

Figure 1.5 Typical coverage of Canada from a 31-horn MBA. Each circle represents the footprint of a specific horn of the antenna.

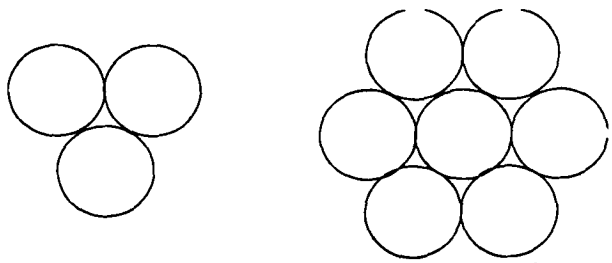

Figure 1.6 Feed horn cluster for a 3- and 7-beam MBA

It can then be appreciated that PA antennas, as well as MBA, present some demanding requirements not found in conventional antennas. These requirements may be broken in three partially overlapping groups; 1) signal distribution 2) signal processing and 3) signal conditioning.

1. Signal Distribution. The large number of elements found in PA antennas and MBAs renders the signal distribution network somewhat more complex. In PAs, the signal must be split, distributed and connected to potentially thousands of elements. Size, weight, signal attenuation and the complexity of the topology become an issue. Implementation of PA and MBA antennas have been slow to date due to the lack of low cost, small size, light weight, low attenuation and high frequency distribution media. Table 1.1 shows a weight, size and attenuation comparison between different distribution media for a 5.3 GHz link and Fig. 1.7 shows a distribution network designed and fabricated for a 18 element MBA using waveguides [1.1].

Conventional microwave systems, using waveguide and coaxial cables are clearly not be suitable for large antennas. Waveguides provide a low loss medium but tend to be bulky and heavy. Coaxial cables, on the other hand, are lighter and more flexible but at the expense of much higher propagation loss and lower phase accuracy. Moreover, these methods do not lend themselves to monolithic fabrication and automated assembly required to lower the total cost of the antenna.

Table 1.1 Weight and size comparison between possible distribution media for a 5.3 GHz link.

Transmission media	Outside Dimension (mm)	Weight (kg / 100 m)	Attenuation (dB / 100 m)
Aluminium rectangular (WR-187)	25 x 50	63	4
Semi-rigid Coaxial Cable (UT250)	6.35	15	53
Fiber Optics	0.25	3.0	0.02

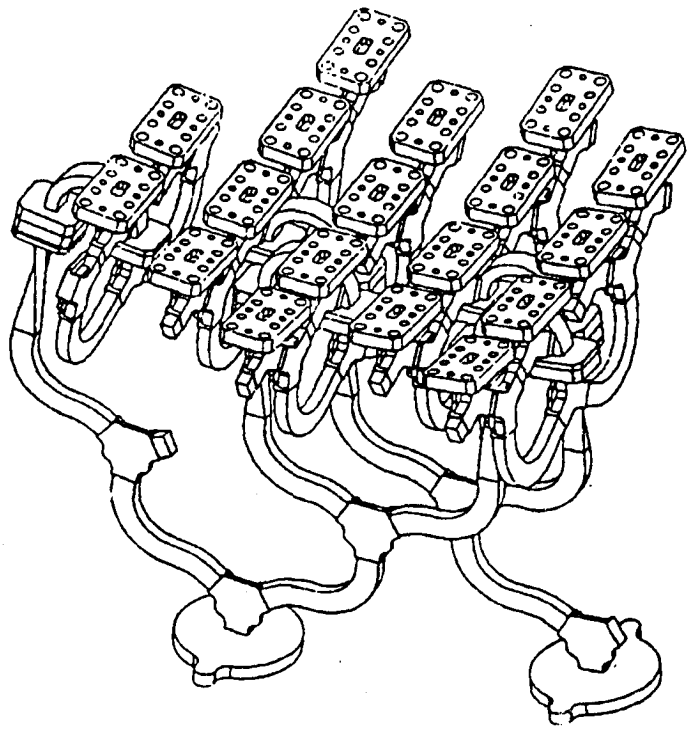

Figure 1.7 Distribution network for an 18 element MBA [1.2].

2. Signal Processing. To allow rapid beam steering and nulling capability, the phase and amplitude weights must be calculated in real time for each element of the antenna. This may involve calculation of the covariance matrix, processing the resulting matrix to determine the complex weights, calculation of two dimensional Fourier transforms etc. Signal processing technology certainly constitutes a booming field but the requirements for beam steering and nulling are considerable. Nulling algorithms usually require N^2 cross-correlations of the signals received from the N antenna elements. These N^2 correlations are usually done in hardware and their values processed according to some algorithm such as matrix inversion, gradient methods. Thus the complexity of determining the weights can be a considerable task for large N.

3. Signal Conditioning. Once the weights have been calculated, they must be applied to the individual element outputs to obtain the desired beam profile. These weights may involve applications of phase shifts, time delays, attenuations, and switching on the signal. Again, for large arrays, the hardware demand may be excessive for practical implementation. Moreover, to obtain the required beam steering accuracy or beam nulling depth, very accurate conditioning is needed, (Variations of less than 1° in phase and less than 0.5 dB in amplitude across the antenna aperture are required for some applications). At microwave frequencies, this accuracy may not always be possible to achieve, especially with large bandwidth signals. Amplifiers, mixers, switches, splitters, attenuators, are all elements of the conditioning electronics which are susceptible to cause erratic variations of the phase and amplitude, due to the fabrication process or due to temperature variations. Table 1.2 shows the number of devices that require stringent amplitude and phase tracking per antenna element in a 44 GHz MBA [1.2]. The first column assumes that conditioning was done entirely at the RF level, while the second column assumes an initial down conversion stage to IF and then signal conditioning. The third and fourth column repeat the experiment but using optical conditioning techniques. It is seen that conditioning at microwave frequencies puts stringent requirements on the electronics.

Table 1.2 Number of matched devices required per channel [1.2]

Unit	Microwave		Optical	
	RF	IF	RF	IF
LNA	1	1	1	1
Mixer	0	1	0	1
IF Amp	0	1	0	1
Modulator	0	0	1	1
Switches	2-6	2-6	0	0
Splitter	1	1	0	0
Attenuators	2	2	0	0
Summer	1	1	0	0
Total	7-11	9-13	2	4

Opto-electronic technologies are being proposed as an alternative for some of the tasks. For example, fibre optics could replace the conventional waveguides or coaxial cables for signal distribution. This replacement would not only reduce considerably the weight and size of the system, as shown in Table 1.1, but would also allow a more flexible distribution medium, lower losses in the signal distribution, better interference immunity, and higher bandwidth. Some of the signal processing tasks could take advantage of the parallel processing capabilities of optical systems. For example, two-dimensional Fourier transforms, and covariance matrix calculations, used to compute the necessary phase and amplitude weighting, could be executed in real time with optics. Moreover, optical technology has the potential of allowing integration with MMIC components. Application of the phase, amplitude or time delay weights could be performed optically. Signal switching to excite the appropriate antenna elements could also be performed using optical technology. Also, as shown in Table 1.2, optical signal conditioning is less susceptible to phase and amplitude variations due to the electronics components.

An idealized block diagram of an opto-electronic implementation of an antenna array is shown in Fig. 1.8. During transmission, the microwave signal, along with the data, are converted to an optical carrier

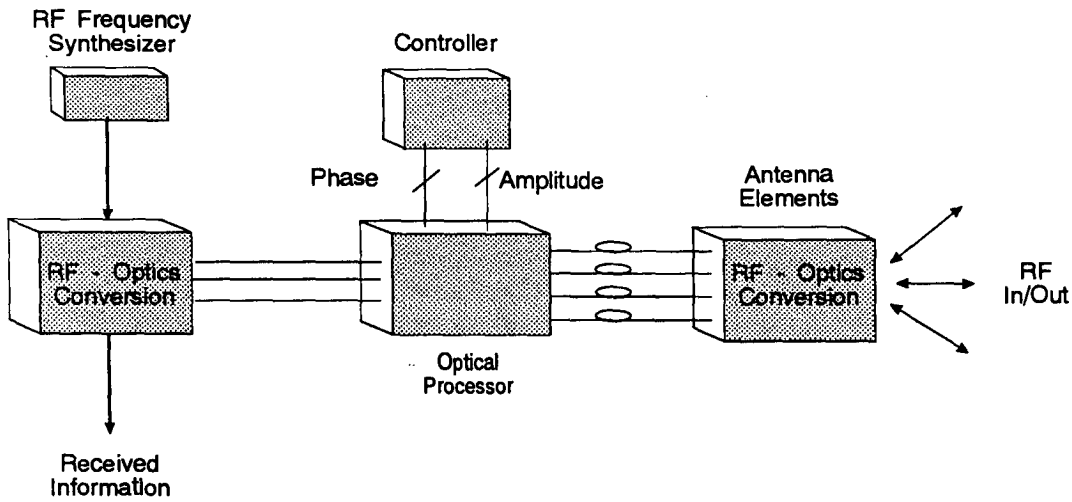

Figure 1.8 Generic block diagram of an electro-optic array antenna implementation.

using intensity or frequency modulation. Phase and amplitude weights, or switching, are impressed on the optical carrier in the optical processor, based on the commands issued by the controller. The processor may be composed of discrete elements such as modulators, attenuators, or more complex systems, such as interferometers and holograms. A fiber optic guiding network then distributes the signal to the proper element of the antenna, where the optical signal is converted back to RF for transmission.

On reception, the RF signal is converted to optics and carried back to the optical processor via fiber optics. Phase and amplitude weighting are also applied to null certain part of the received signal. Finally, conversion back to an electrical signal is done.

As seen, an electro-optic implementation of an array antenna will incorporate four functions using optical technology:

1. RF-to-optics conversion
2. Processing (phase, amplitude and time delay weighting)
3. Signal distribution
4. Optics-to-RF conversion

The technique used to implement these functions may vary widely depending on the antenna frequency of operation, number of elements, processing complexity, etc.

In this report, each of these functions is reviewed. Different implementation strategies are proposed and evaluated. Chapters 2 and 3 are concerned with the conversion of the RF signal to and from an optical carrier respectively. Chapter 4 serves to describe various beam forming techniques or methods to apply phase and amplitude weights to the signal in a desired direction. Chapter 5 is devoted to the signal distribution aspect including an optical power budget.

2.0 RF-to-OPTICS CONVERSION

The conversion of the electrical signal, either received or to be transmitted, to the optical domain is generally done by modulating the amplitude or the frequency of an optical signal. There are basically three conversion methods: direct, external and heterodyne. Direct modulation, only applicable to semiconductor diode lasers or light emitting diodes, involves a variation of the diode's bias current at the desired microwave frequency. This current variation may translate into a variation of the optical output intensity or may be used to frequency shift the optical signal. External modulation, as its name implies, involves a modulator external to the laser. This approach is not limited only to semiconductor lasers but may be used also with other types of lasers such as the gas or solid state. The optical signal is focused in a device where it is phase, frequency or intensity modulated by an acoustic or electro-magnetic effects produced by the RF signal to convert. The heterodyne technique, on the other hand, is based on the mixing of two optical signals in a photodetector to produce a beat frequency equal to the frequency separation between these optical signals.

In this section, these three conversion techniques are analyzed. A general description of each is given and an evaluation of their applicability to the system is given. However, before proceeding with the analysis of the modulation techniques, a brief review of the main characteristics of the potential optical sources is given.

2.1 OPTICAL SOURCES

The optical source represents the direct link between the electrical and the optical portions of the system. It provides the optical power which, after being modulated and conditioned, is distributed to each element via fiber optic. Optical sources will most often be in the form of light emitting diodes (LEDs) or lasers. Other types of light sources such as tungsten lamps, arc lamps, are to bulky and not reliable enough to be used in real systems.

LEDs are small, low power (less than 3mW) and inexpensive (a few cents) light sources operating on the principle of electroluminescence. Direct modulation is the usual modulation technique. The optical wavelength may vary from 0.4 to 1.3 μm. Since attenuation in fiber optic is wavelength dependant, the LED chosen will greatly influence the optical power distribution efficiency. LEDs have extremely wide linewidth (2000 GHz) and are consequently not suitable for heterodyne techniques.

Lasers are somewhat more complex but offer some very interesting characteristics, as will be shown. There are basically three types of lasers for the application: the well known gas lasers such as He-Ne, the high performance solid state lasers (e.g.Nd:YAG) and the semiconductor laser diodes, such as those based on GaAlAs, InGaAs, and InGaAsP.

The gas laser, principally the red emitting (.633 μm) He-Ne, is established on a well understood technology, has a very narrow spectral profile, outputs a single mode beam, and has minimal temperature dependency. Furthermore, since He-Ne lase in the visible region (red light at 0.633 μm) they can greatly simplify the system alignment procedures. However, gas lasers suffer from several drawbacks. For one, they tend to be bulky and are inefficient in terms of electrical to optical power conversion. For example, a 15 mW He-Ne measures approximately 15 cm long and requires some 250 W of electrical power, i.e less than 0.01% conversion efficiency. Another disadvantage of He-Ne is the high propagation losses exhibited in fiber optic, (approximately 7 dB/km) which precludes them from being used on long haul or in systems where power is limited.

The Nd:YAG laser operates in the near infrared region (1.06μm), consequently is invisible. It presents a low fiber attenuation (0.1dB/km). In addition, its narrow spectrum linewidth (better than 10kHz) makes it an excellent candidate for heterodyne systems. Sufficient coherent output power may be obtained for most signal processing and signal distribution applications. Commercially available Nd:YAG lasers have CW output powers in the range of 10 to 600 mW. However, the main disadvantage with Nd:YAG lasers is their greater complexity when compared to laser diodes, and their low conversion efficiency.

Semiconductor lasers are divided into two groups, based on the fabrication material and the lasing wavelength. The GaAs / GaAlAs lasers operate around 0.85μm and the InGaAs / InGaAsP diodes operate in the 1.3-1.5 μm. The CD ROM technology is pushing the short wavelength lasers whereas the fiber optic communication community is pushing for the longer wavelength. At this time, the technology around the laser (modulators, fiber optics, detectors...) favours the longer wavelength. However, to maximize the integration process and lower the cost, GaAlAs lasers would be preferred since the RF section will most likely be built around GaAs MMIC.

Table 2.1 summarizes the characteristics of some optical sources which could be used.

Table 2.1 Characteristics of a number of potential candidate for laser source.

SOURCE	λ (μm)	POWER	LINEWIDTH	MODULATION	FIBER ATTENUATION (dB/km)	EFFICIENCY ELECTRICAL-OPTICAL
LED	0.4-1.3	3 mW	20000 GHz	Dir	--[1]	5%
He-Ne	0.633	5 mW	450 MHz	Ext	7	0.01%
GaAlAs	0.780 - 0.850	30 mW	10 MHz	Dir / Ext	2	30%
Nd:YAG	1.064/ 1.3	1 W	<10 kHz	Ext	0.1 / 0.02	4%
InGaAs	1.3	5 mW	10 MHz	Dir / Ext	0.02	30%
InGaAsP	1.5	5 mW	10 MHz	Dir / Ext	0.01	30%

Dir = Direct, Ext = External
[1] Wavelength dependent

2.2 DIRECT MODULATION

This technique is applicable only to the semiconductor laser diodes or to the light emitting diodes. In this section, the word "diode" will be used to identify either one. If comments apply only to one type, qualifiers will be added.

In a direct modulation implementation, the RF signal is added to the DC bias current of the diode (laser or light emitting) as shown in Fig. 2.1. Since the output power of diodes is proportional to the bias current, a variation of that current produces an intensity modulated output signal as seen in Fig. 2.2.

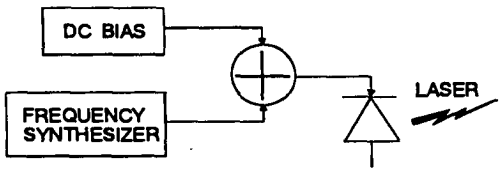

Figure 2.1 A typical direct modulation implementation where the RF signal is added to the DC bias current of the diode.

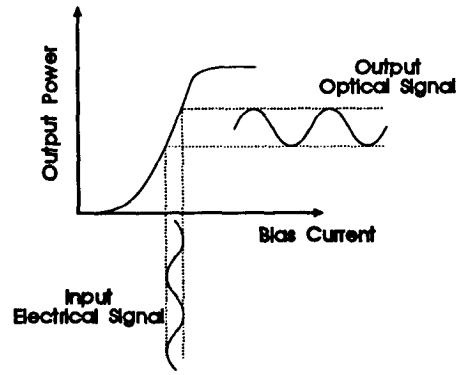

Figure 2.2 Typical conversion curve from electrical bias current signal to optical output power

Although this implementation is rather simple, its major drawback resides in the limited modulating bandwidth achievable. Fig. 2.3 shows a typical normalized-amplitude response of a diode as a function of the modulating frequency [2.1]. The measured response is typically flat for low modulating frequencies, but suddenly changes to a 40 dB/decade roll-off after a resonant frequency peak. To a first approximation, the resonance frequency is given by [2.2]:

$$f_r = \frac{1}{2\pi}\sqrt{\frac{AS_o}{\tau_r}} \qquad (2.1)$$

where:

A = optical gain coefficient,
S_o = internal photon density,
τ_p = photon lifetime.

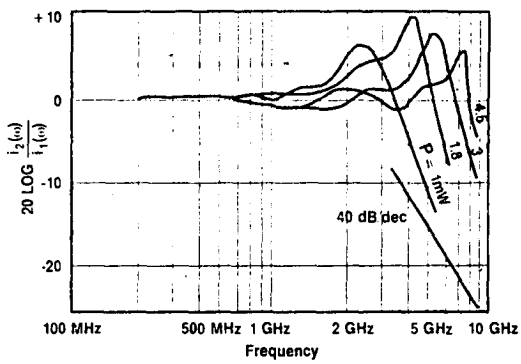

Figure 2.3 Typical normalized direct modulation responses of a GaAs laser diode as a function of the modulating frequency for different output power. [2.1]

The resonant frequency and consequently the useful bandwidth, may be increased by careful adjustments of these three parameters. The gain coefficient A may be increased by cooling the diode; a factor of five may be obtained by lowering the temperature from room to liquid nitrogen (77K). The drawback with this method, apart from the fact that cooling is required, is a decrease in the modulation efficiency due to an increase in the series resistance of the diode which occurs at low temperatures. For laser diodes, the gain may also be increased, by a factor of two, if semiconductor quantum well structures are used instead of the conventional coplanar structure. The photon density S_o may be increased by biasing the diode to higher current, i.e. operating at higher optical power. However, this increment must be limited to prevent catastrophic damage of the laser facets. Finally, the photon lifetime τ_p can be reduced by decreasing the laser cavity length. In this case, thermal effects limit the cavity reduction and hence the bandwidth.

In Ref. 2.6, a technique, involving mode locking, is described to modulate a laser diode at frequency much higher than the relaxation frequency. By using an "external resonating cavity", tuned to the desired RF frequency (Fig. 2.4), the laser mode will lock on the resonating frequency of the cavity generating a optical pulse train at the RF frequency. The RF-to-optics conversion efficiency may be improved by some 12 dB using this mode locking approach [2.6]. Note that mode locking only produces a pulse train which could be sufficient to lock a microwave oscillator. In 2.6, the information was put on the mode-locked optical signal using a external modulator. A 20 GHz centre frequency RF signal with a 2 GHz bandwidth was converted on an optical carrier using this technique [2.6].

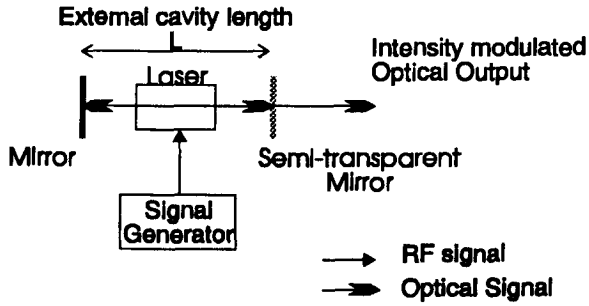

Figure 2.4 Schematic diagram of a laser diode direct modulation technique using an external cavity to increase the maximum modulation frequency.

Table 2.2 shows some typical values of maximum direct modulation frequencies for various types of diodes. At the lower end, there are the light emitting diodes with a maximum modulation frequency of approximately 150 MHz. For laser diodes, this frequency is much higher. Typically, the resonant frequency for the short wavelength diode lasers (GaAs) are below 6 GHz. A 12 GHz bandwidth 0.8 μm (GaAlAs) laser was available from Ortel but was discontinued in 1990 [2.3] due to the small demand. Laboratory experimental multiple quantum wells GaAlAs lasers have been demonstrated with a bandwidth up to 30 GHz [2.4]. On the other hand, lasers in the longer wavelength region, around 1.3 - 1.5 μm, are commercially available with modulation bandwidth of 12 GHz [2.5].

Table 2.2 Maximum direct modulation frequency of various types of semiconductor diodes

Diode Type	Optical Wavelength	Maximum Modulating Frequency	Observations
Light Emitting Diode	400-1300 nm	150 MHz	Commercially available
AlGaAs laser	780-930 nm	4 GHz	Commercially available
AlGaAs laser	800 nm	12 GHz	Ortel [2.3], discontinued in 1990, no longer available.
InGaAsP	1500 nm	12 GHz	Commercially available.

Apart from modulating the intensity of the optical signal, direct modulation of semiconductor laser diodes, may also be used for frequency modulating the optical signal. Fig. 2.2 showed that a variation of the laser diode bias current creates a variation of the optical signal intensity. This bias current variation will also create a variation in the optical wavelength. Typical wavelength deviation is in the order of a 3GHz/mA. This variation of the optical wavelength becomes similar to a frequency modulation. From the theory of amplitude and frequency modulation, one can write the resulting electric field of the light beam resulting from the superimposition of a modulating sinusoidal signal at a frequency f_m on the DC bias current of the laser diode as [2.7]:

$$E(t) = E_0 [1+M\cos(2\pi f_m t)] \cos(2\pi f_c t + \beta \sin(2\pi f_m t))] \quad (2.2)$$

where:

f_c = laser centre frequency
f_m = RF modulation frequency
β = frequency modulation index $\Delta F/f_m$
ΔF = maximum frequency deviation (which depends on the amplitude of the bias current variation)
M = amplitude modulation index.

The frequency modulation is easily seen from the expression of the instantaneous frequency given by:

$$f = f_c + \Delta F \cos(2\pi f_m t) \quad (2.3)$$

Expanding Eqn. 2.2 in terms of Bessel functions of the first kind (Eqn. 2.4), it may be seen that the optical signal has several sidebands spaced by f_m on each side of the optical carrier frequency f_c. The intensity of these sidebands are given by the square of the coefficient corresponding to the sideband of interest in Eqn. 2.4. Fig. 2.5 shows the maximum intensity achievable by anyone of the first 10 harmonics. A modulation index of 0.4 has been assumed and the frequency modulation index β has been chosen for each harmonic to maximize the intensity.

$$
\begin{aligned}
E = {} & J_0(\beta)E_0 \cos(\omega_c t) \\
& + \{J_1(\beta) + (\frac{M}{2})[J_0(\beta) + J_2(\beta)]\}\ E_0 \cos(2\pi(f_c+f_m)t) \\
& + \{-J_1(\beta) + (\frac{M}{2})[J_0(\beta) + J_2(\beta)]\}\ E_0 \cos(2\pi(f_c-f_m)t) \\
& + \sum_{n=2}^{\infty} \{J_n(\beta) + (\frac{M}{2})[J_{(n-1)}(\beta)+J_{(n+1)}(\beta)]\}\ E_0 \cos[2\pi(f_c+n*f_m)t] \\
& - \sum_{n=2}^{\infty} \{+J_n(\beta) + (\frac{M}{2})[J_{(n-1)}(\beta)+J_{(n+1)}(\beta)]\}\ E_0 \cos[2\pi(f_c-n*f_m)t]
\end{aligned}
\tag{2.4}
$$

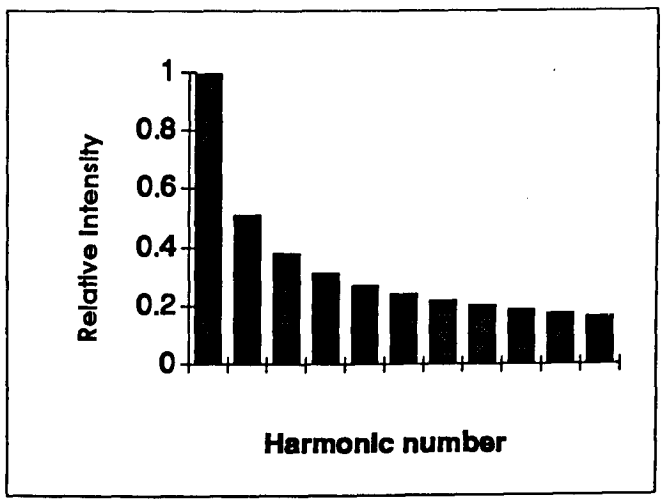

Figure 2.5 Maximum intensity of harmonics resulting from amplitude modulation. Amplitude modulation index set to 0.4 and frequency deviation index chosen, for each harmonics, to maximize the intensity.

2.3 EXTERNAL MODULATION

External modulators may be used with any of the optical sources mentioned; LEDs, semiconductor, gas, or solid state lasers. There are two main groups of external modulators classified according to the interaction between the RF signal and the light wave: acousto-optic and electro-optic.

2.3.1 Acousto-optic modulator

Acousto-optic (A-O) modulators operate from the interaction between an acoustic wave and the optical beam [2.8,2.9]. The acoustic wave is generated in a crystal (e.g. $LiNbO_3$, TeO_2, SiO_2) by a piezoelectric transducer excited by the RF signal. The optical signal, emerging from the A-O modulator, is diffracted at an angle, θ_B, proportional to λ/Λ where λ and Λ are the optical and acoustic wavelengths respectively. The optical frequency is also shifted by an amount equal to the electrical signal frequency. The A-O modulator may then be used as an amplitude or frequency modulator.

An interesting characteristic of acousto-optic modulators, when operated in the Raman-Nath regime (rather than in the Bragg regime) is their ability to generate multiple orders of diffracted beams; which corresponds to frequency shifts of harmonics of the driving signal. The Raman-Nath diffraction occurs at relatively low frequencies when the acoustic beam width along the optical propagation direction is small. In this regime the diffracted light appears symmetrically on both sides of the primary beam at equally spaced angles proportional to $m\lambda/\Lambda$, where m is an integer representing the diffraction order. The optical frequency is, at the same time, shifted by an amount equal to $\pm m\ \omega_a$, where ω_a is the input driving signal frequency.

The main drawback with A-O modulators is their limited bandwidth. Most of the commercially available A-O cells have bandwidths of the order of a few hundred MHz with some achieving 2 GHz [Brimrose model TEM-170-30]. Laboratory prototypes having bandwidth of 8 GHz have been demonstrated but are not commercially available.

2.3.2 Electro-optic modulator

Electro-optic modulators capitalize on the fact that the refractive index of a crystal changes when an electric field is applied. When the relation between the index and the electric field is linear, the electro-optic effect is called the Pockels effect. If the relation is quadratic (the refractive index changes as the square of the applied field) it is called the Kerr effect. Most of the light modulators operate in the linear region, thus under the Pockels regime. The refractive index variation, induced by the applied RF signal, is then put to profit to induce a phase shift (resulting from the variation of the propagation speed of the light wave in the waveguide) or to couple the optical signal into a different path. Phase, frequency and amplitude modulations may thus be achieved.

2.3.2.1 Phase modulator

A typical phase modulator is depicted in Fig. 2.6. A voltage V is applied to the electrodes placed over or alongside a waveguide in which the optical beam is propagating. The internal electric field generated has an approximate magnitude of $|E| \approx V/G$ where G is the electrode gap. Due to the linear electro-optic (Pockels) effect, the refractive index of the waveguide is altered, and the variation may be expressed by the relation [2.10]:

$$\Delta n = -\frac{n^3}{2} r \Gamma \frac{V}{G} \qquad (2.5)$$

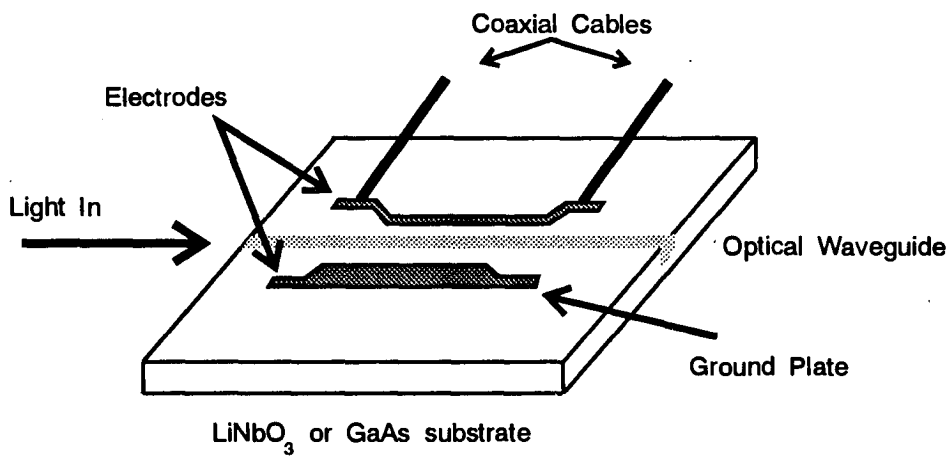

Figure 2.6 Schematic view of an integrated-optics phase modulator.

where :

n = index of refraction of the material
r = Pockels constant
G = electrode gap
V = drive voltage applied to the electrodes
Γ = overlap integral between the applied electric field and the optical mode

$$\Gamma = \frac{G}{V} \iint E\,|E'|^2\,dA$$

E = applied electric field
E' = normalized optical field distribution

Consequently, the optical phase shift, $\Delta\phi$, incurred over an interaction length L may be expressed as:

$$\Delta\phi_0 = 2\pi\Delta n\frac{L}{\lambda} = -\pi n^3 r\,\Gamma\,\frac{V}{G}\,\frac{L}{\lambda} \tag{2.6}$$

As a numerical example, consider a phase modulator built on $LiNbO_3$ ($r=30.8\times10^{-6}$ μm/V, $n_e = 2.2$), with G equals 5 μm, a Γ of 0.3 and an interaction length L of 10 mm. With an optical wavelength of 0.8 μm, a voltage of 4.1 V would be required to induce a 180° phase shift of the optical signal.

The above equation is to be taken only as a first approximation. It assumes that the light wave will travel down the optical waveguide at the same velocity as the microwave drive signal along the electrodes. Consequently, the optical signal would see the same voltage over the entire waveguide. In practice, there is always some velocity mismatch between the optical and electrical signals. This difference leads to a reduction or cancellation of the phase shift for arbitrarily large L or drive signal frequency. The correct equation for the actual phase shift should be [2.11]:

$$\Delta\phi = \Delta\phi_0\frac{\sin(\psi/2)}{(\psi/2)}\sin(\psi/2 - 2\pi f t_0) \tag{2.7}$$

where:

ψ = $\pi f/f_c$
f = microwave signal frequency

$$f_c = \frac{c}{2\,N_m\,L\,\delta}$$

c = 3×10^8 m/s
N_m = refractive index at microwave frequency
$N_m = 4.2$ for $LiNbO_3$ and $N_m = 3.9$ for GaAs
δ = a measure of the velocity mismatch between the optical and microwave signals equals to $1-N_0/N_m$,
N_0 = refractive index at optical frequencies
$N_0 = 2.2$ for $LiNbO_3$ and $N_0 = 3.6$ for GaAs

For $N_0 = N_m$, the optical wave travels down the waveguide at the same speed as the RF signal travels the electrode and "sees" the same voltage over the entire electrode length. However, if $N_0 \neq N_m$, which is the usual condition, there is a walk-off between the optical wave and the microwave drive signal. If the electrode length is sufficiently long, or if the microwave frequency is large, there could be a cancellation of the phase shift. The microwave frequency for which the optical phase shift is reduced to 50% of its value if a DC level were used (f = 0) is:

$$\Delta f = \frac{2c}{\pi N_m \delta L} \tag{2.8}$$

This shows that the achievable bandwidth is critically dependant on the velocity mismatch between the electrical and optical signals for a given electrode length. With a reduced interaction length, faster operation may be achieved, but at the expense of higher drive power (proportional to 1/L).

For example, using the parameters given above, the bandwidth-length product for a $LiNbO_3$ waveguide is 9.42 GHz-cm. For a GaAs waveguide the product would be 63.6 GHz-cm.

A great deal of effort has been put into devising configurations in which the velocity mismatch would be reduced. Among those we may note:

- Travelling-wave with coplanar electrodes,
- use of shielding ground planes above coplanar strips,
- periodic loading of the capacitance between modulator electrodes,
- sequential reversal (aperiodic or coded reversal) of the modulation polarity,
- use of band operation,
- tandem operation.

It is beyond the scope of this report, to describe each one, but the interested readers may consult references 2.12 and 2.13.

2.3.2.2 Frequency modulator

A phase modulator may also be used to perform frequency translation [2.14]. Equations 2.2 and 2.4 showed that frequency sidebands appears in the spectrum of a phase modulated signal. Consequently, if the RF input of an optical phase modulator is equal to $\beta\sin(2\pi f_{RF}t)$, the output optical signal will present sidebands separated by f_{RF} with relative amplitude depending on the modulation index β. When two phase modulators in parallel, it becomes possible to eliminate all even harmonics and when four modulators are used, a single sideband frequency translator may be produced [2.15, 2.16]. Fig. 2.7 gives a schematic representation of a two-arm optical frequency translator.

A single-mode laser is used as CW light source. The light is injected in a single mode waveguide for propagation to a beam splitter. The configuration of these two arms is essentially identical to a Mach-Zehnder interferometer except that in this case both arms must be accessible and the optical phase shift excursion must be done over 2π radians. If $\beta_1 = \beta_2$, upon recombination, the electric field takes the form of:

$$A(t) \sum_{n=-\infty}^{\infty} J_n(\beta) \cos\left[(\omega_c + n\,\omega_m)\, t \right] \cos\left[\frac{1}{2}\left(\Delta\phi_c + n\,\Delta\phi_m \right)\right] \tag{2.9}$$

where

A(t) is the amplitude of the optical signal
β the modulation index
ω_c, ω_{rf} the optical and RF angular frequency
$\Delta\phi_c$ the optical phase difference between the two arms of the interferometer
$\Delta\phi_{rf}$ the RF phase difference between the two phase modulators.

From Eqn. 2.9, it is seen that to maximize the first harmonics $\omega_c \pm \omega_{rf}$, we must set $\beta = 1.84$, $\Delta\phi_c = \Delta\phi_{rf} = \pi$,. To maximize for the second harmonic $\omega_c \pm 2\omega_{rf}$, we must set $\beta = 3.052$, $\Delta\phi_c = \pi$, $\Delta\phi_{rf} = \pi/2$.

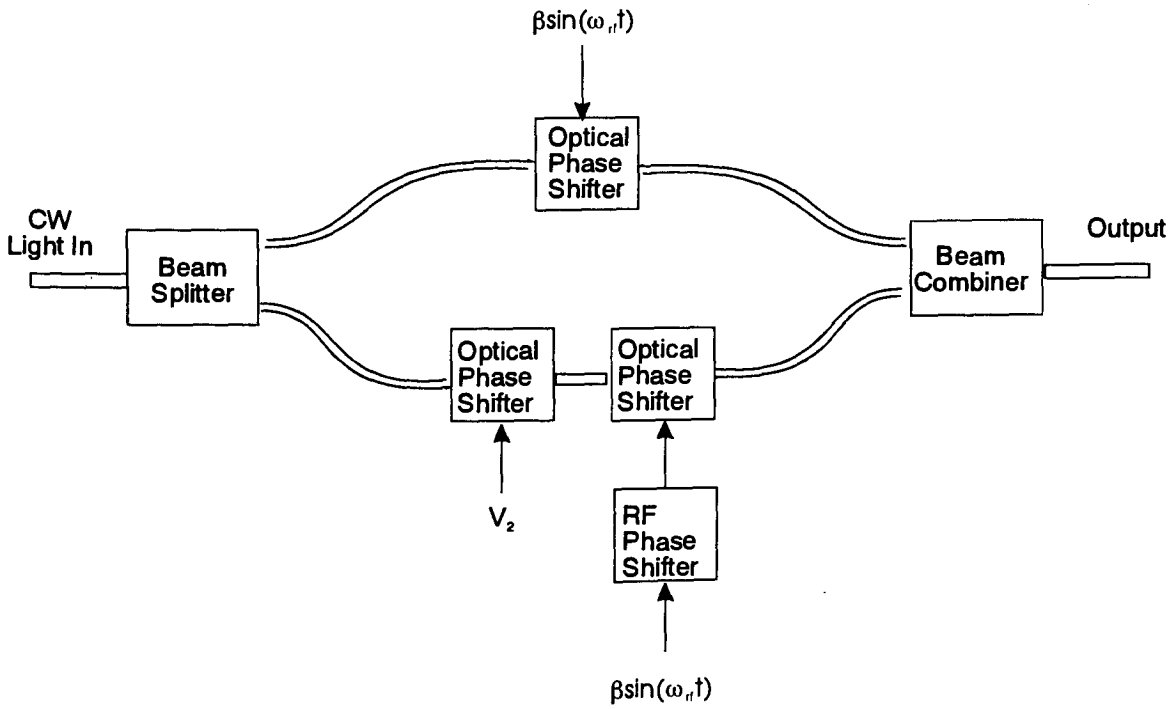

Figure 2.7 Schematic representation of a two-arm frequency translator.

2.3.2.3 Intensity modulator

Several construction techniques may be used to devise an electro-optic intensity modulator. The most common ones are:

a. Directional coupler,
b. Interferometric modulator
   - Mach-Zehnder type,
   - Crossed-Nicol type,
   - Push-Pull type,
c. Cut-off modulator.

The most popular external intensity modulators are the directional coupler and the Mach-Zehnder interferometers. They are pictured in Fig. 2.8

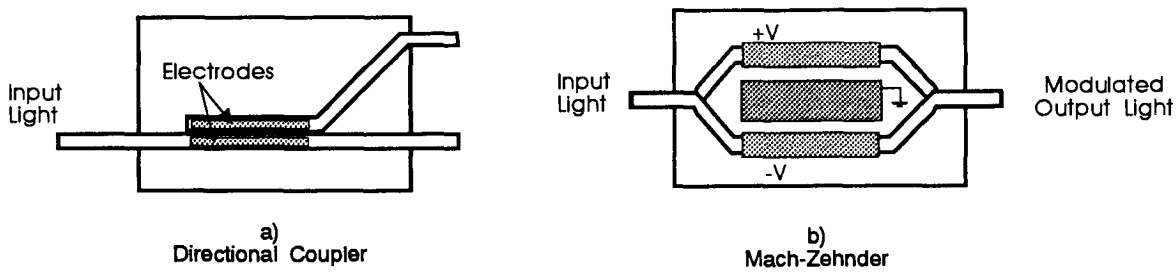

Figure 2.8 Two popular external intensity modulators. a) directional coupler b) Mach-Zehnder interferometer.

2.3.2.3.1 Directional Coupler. If two waveguides are sufficiently close together such that their fields overlap, it is possible to transfer the optical power from one waveguide to the other. The exact analysis of the interaction involves manipulations of Maxwell's equations, which is far beyond the scope of this report. Without going into the mathematical details, it can be shown that, for weak coupling, the optical power in each collinear waveguide, as a function of the distance, can be expressed as [2.17]:

$$P_1(L) = P_1(0)\left[\cos^2(\gamma z) + \left(\frac{\Delta\beta}{2\gamma}\right)^2 \sin^2(\gamma z)\right]$$

$$P_2(L) = P_1(0)\left[\frac{|\zeta|^2}{\gamma^2}\sin^2(\gamma z)\right] \qquad (2.10)$$

where

$P_1(0)$ = optical power input in the first waveguide

$\Delta\beta$ = phase mismatch per unit length between the modes propagating in each waveguide

$$= \frac{2\pi\Delta n}{\lambda_0}$$

Δn = refractive index difference between the two waveguides

ζ = coupling coefficient between the waveguides; depends on the refractive indexes, dimensions, separations.

$$\gamma = \sqrt{\left(\frac{\Delta\beta}{2}\right)^2 + \zeta^2}$$

Fig. 2.9 shows the power exchange between two identical waveguides, i.e. $n_1 = n_2$, $\Delta\beta = 0$.

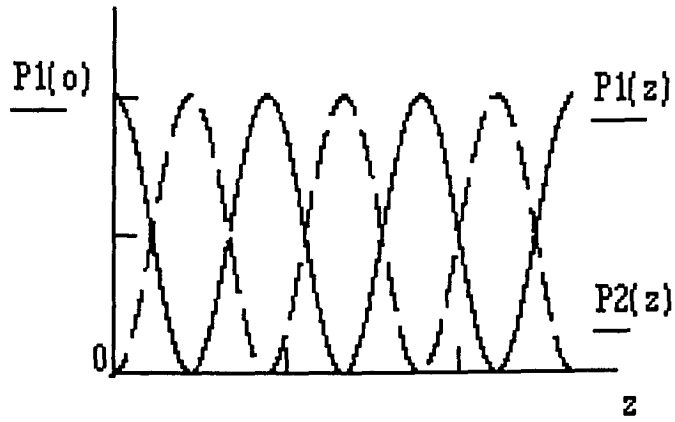

Figure 2.9 Power exchange between waveguides 1 and 2 when the refractive index are identical, i.e $\Delta\beta = 0$.

The distance for which the power is completely transferred from one waveguide to the other is called the coupling length L_0 . The value of L_0 largely depends on the geometry of the waveguides. Typical values range from a few millimetres to a few centimetres. The closer the waveguides are, the shorter the coupling distance.

Assuming that the waveguides overlap over the coupling distance L_0, it can be shown that the power-transfer ratio $\Psi = P_2(L_0)/P_1(0)$ may be written as [2.18]:

$$\Psi = \frac{P_2(L_0)}{P_1(0)} = \left(\frac{\pi}{2}\right)^2 sinc^2\left(\frac{1}{2}\left[1+\left(\frac{\Delta\beta L_0}{\pi}\right)^2\right]^{\frac{1}{2}}\right) \tag{2.13}$$

Fig. 2.10 illustrates the dependence of the power-transfer ratio on the phase mismatch parameter $\Delta\beta L_0$.

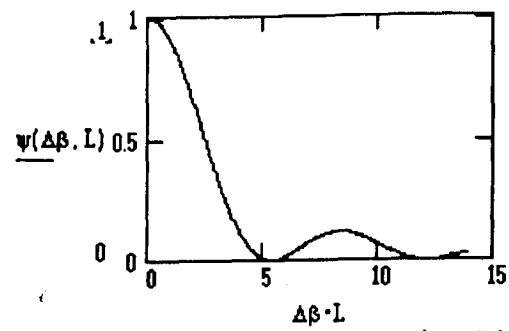

Figure 2.10 Dependence of the power transfer ratio on the phase mismatch parameter.

The ratio has its maximum value, i.e. complete optical power transfer from waveguide 1 to waveguide 2, when $\Delta\beta L_0 = 0$, and its minimum at $\sqrt{3}\pi$, where no power is transferred to waveguide 2. Consequently, by controlling $\Delta\beta$ it becomes possible to control the power transfer from one waveguide to the next, to perform intensity modulation. Control of $\Delta\beta$ may be electrically achieved if the refractive index of the material can be altered by an electric field. Using Eqn. 2.5 in the definition of $\Delta\beta$, it is found that the necessary voltage required to prevent the optical power from transferring from waveguide 1 to waveguide 2, when the two waveguides have, originally, the same refractive index, is:

When V = 0, all of the optical power from waveguide 1 is coupled into waveguide 2 at a distance of L_0. When the applied voltage is equal to V_0, no power is transferred. Switching voltages are typically under 10 volts.

2.3.2.3.2 Mach-Zehnder Interferometer. This type of modulator also achieves intensity modulation but, using waveform interference. As shown in Fig. 2.8, the input light is divided into equal components, using a 50/50 directional coupler configuration. By applying a voltage to the electrodes of one arm, a phase shift between the two optical signals can be created. Upon recombination, intensity modulation may be obtained depending on the relative phase shift applied. A differential phase shift of 180° will result in a minimum output amplitude whereas if the two beams recombine in phase, the full signal intensity will result. The intensity modulated output I, in a Mach-Zehnder type modulator, is given by:

$$I = I_0 \cos^2\left(\frac{\Delta\beta\, L_0}{2}\right) \tag{2.11}$$

By shifting the phases of each arm in opposite directions, a relative phase shift of 180° (and consequently a null in the output intensity) may be obtained with half the voltage needed in the phase modulator (Eqn. 2.6).

The extinction ratio, i.e. the ratio between the maximum output power ($\Delta\phi$=0°) and the minimum output power ($\Delta\phi$=180°) may be expressed as [2.19]:

$$E_r = 10\log\left[\frac{(1+\sqrt{r_p})}{(1-\sqrt{r_p})}\right]^2 \; dB \tag{2.12}$$

where r_p is the power division ratio between the two arms. For example, suppose a typical power splitting ratio r_p of 1.2, and the conditions given in the previous section. From Eqn. 2.5, the required voltage would drop to 2.05 V (since two electrodes of reverse polarity are used) and the extinction ratio would be 15 dB.

2.3.2.4 Design considerations of external modulators

External modulators, based on integrated-optics techniques, may be fabricated from a number of materials. Table 2.3 gives the characteristics of some of them. The most popular are $LiNbO_3$ and GaAs. $LiNbO_3$ is a well established technology for modulators. The waveguide is transparent to wavelengths from 0.4 to 5 μm which makes it an excellent candidate for a large number of applications. It is widely used in the fiber optic communication field. It has high electro-optic coefficients which allow low RF drive voltages. Moreover, the interfacing with monomode fiber optic is made simple since the modal sizes are similar. In a standard travelling-wave configuration, the bandwidth-length product is in the order of 9 GHz-cm. On the other hand, modulators based on GaAs are compatible with opto-electronic integration. Compact waveguides are possible, which makes the electro-optic interaction very efficient. They also allow for very

wide bandwidth with low RF drive requirements when the travelling wave configuration is used. Their bandwidth-length product may reach up to 60 GHz-cm in the standard travelling wave configuration. However, GaAs based modulators, have a higher wavelength range, from 0.9 μm to 16 μm.

Table 2.4 gives some of the best reported results obtained with integrated electro-optics modulators. Table 2.5 gives the performance of some commercially available E-O modulators.

Table 2.3 Characteristics of some material used in the fabrication of electro-optic modulators

Crystal	Pockels Constant $r_{33} \times 10^{-12}$ (m/V)	Refractive Index	Wavelength Transparency (μm)
$LiNbO_3$	30.8	$N_0 = 2.286$	0.4 - 5
$LiTaO_3$	30.3	$N_0 = 2.176$	0.45 - 5
GaAs	1.2 (r_{41})	$N_0 = 3.6$	0.9 - 16
ADP ($NH_4H_2PO_4$)	28 (r_{41})	$N_0 = 1.52$	0.19 - 1.5
KDP (KH_2PO_4)	8.6 (r_{41})	$N_0 = 1.51$	0.2 - 1.55

Table 2.4 Reported performance of some optical waveguide modulators.

Author	Description	λ	V_π	Bandwidth (GHZ)
Wakita et al (1990)}[2.20]	InGaAsAs/InAlAs MQW	1550	7	40
Walker (1991)[2.21]	GaAs/AlGaAs TW loaded-line M-Z push-pull	1300	5.75	36.5
Walker, Carter (1988)[2.22]	GaAs/GaAlAs lumped M-Z push-pull	840	4.25	6.25
Korotky et al (1987)[2.23]	Ti:$LiNbO_3$ directional coupler	1560	26	40
Cross et al (1984)[2.24]	Ti:$LiNbO_3$ Traveling-wave Mach-Zehnder	840	2	13
Gee et al (1983)[2.25]	Ti:$LiNbO_3$ Travelling-wave Mach-Zehnder	830	-	17

Table 2.5 Device characteristics of some commercially available E-O modulators.

Company	Model	Type	Bandwidth	Wavelength
Brimrose Technology	TEM-170-30	A-O cell	1.7 GHz ± 300 MHz	400 - 840 nm optimum @ 633nm
British Telecom & Dupont	IOCO100	$LiNbO_3$ Phase Modulator	4 GHz	1300/1550 nm
Crystal Technology, Inc.	MZ385P MZ313P MZ315P	Mach-Zehnder	2.5 GHz	850 nm 1300 nm 1550 nm
Hoechst Celanese	Y-35-8808-01	Mach-Zehnder	18 GHz	1300 nm
United Technology	4537 4538	Mach-Zehnder	18 GHz	1300 nm 1500 nm

2.4 HETERODYNE

Another alternative to convert an electrical signal to an optical signal is by means of a heterodyne technique. This technique, well known in the RF domain, consists in mixing two signals together to generate the sum and difference frequencies. The same principles apply in the optical domain. Two optical signals, separated by some desired microwave frequency, coupled together will generate the sum and difference frequencies as well as the cross products of their harmonics. The basic configuration for optical generation of a microwave signal is shown in Fig. 2.11.

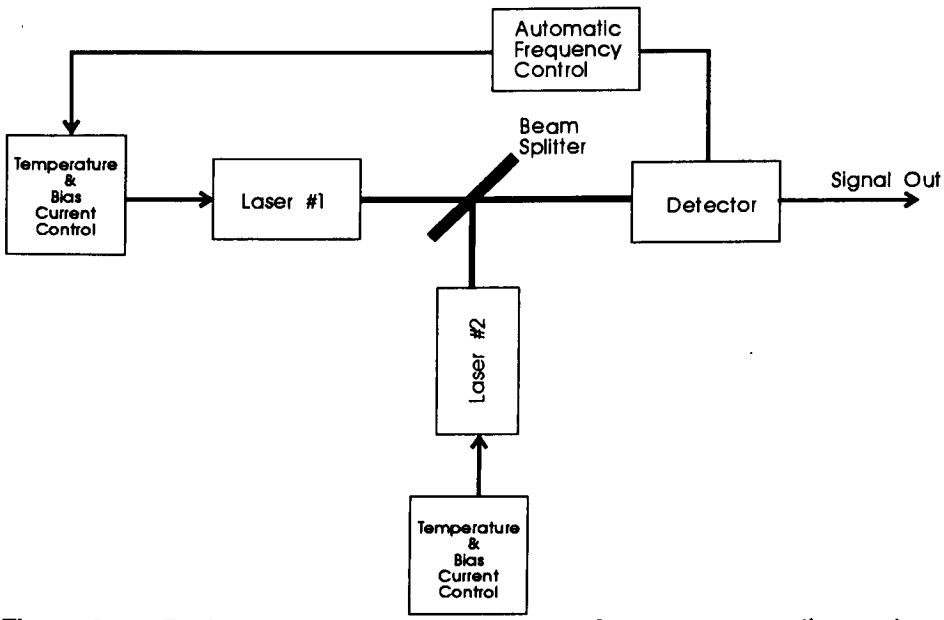

Figure 2.11 Basic configuration of a microwave frequency generation system using optical heterodyne techniques.

Mathematically this process can be expressed as follow. Assume $S_1(t)$ and $S_2(t)$ the light wave signals emitted by each laser, given by the following expressions:

$$S_1(t) = A\cos(2\pi f_1 t + \phi_1(t))$$
$$S_2(t) = B\cos(2\pi f_2 t + \phi_2(t)) \qquad (2.13)$$

where A and B are the respective amplitude of the laser output signals, f_i and $\phi_i(t)$, i=1,2 their frequency and phase. Note that the phase term is time dependent. This term is related to the laser linewidth. Due to intrinsic characteristics of the lasers, the optical signal emitted has a non-zero bandwidth (or linewidth) which causes the optical frequency to rapidly changes about a central frequency and therefore broadening the bandwidth of the signal. Typical bandwidths of laser diodes are in the order of 10 to 50 MHz. Special fabrication techniques or the use of external cavities may reduce this bandwidth to a few kHz but at the expense of a more complex system. Nd:YAG lasers, on the other hand, offers bandwidth in the order of 10 kHz without any compensation techniques.

The photodetector, being a squaring device, will produce an electrical signal proportional to (dropping the gain factor):

$$I(t) = |S_1(t) + S_2(t)|^2$$

$$= \frac{|A|^2}{2} + \frac{|B|^2}{2} + \frac{|A|^2}{2}\cos[2\omega_1 t + 2\phi_1(t)] + \frac{|B|^2}{2}\cos[2\omega_2 t + 2\phi_2(t)] \qquad (2.14)$$

$$+\frac{|A||B|}{2}\cos[(\omega_1+\omega_2)t + (\phi_1(t)+\phi_2(t))] + \frac{|A||B|}{2}\cos[(\omega_1-\omega_2)t + (\phi_1(t)-\phi_2(t))]$$

The electrical signal generated then consists of a DC component, tones at twice the frequency of $S_1(t)$ and $S_2(t)$, one at the sum frequency and one at the difference frequencies. However, due to the limited bandwidth of photodetectors, only the DC component and the signal at the difference frequency will be detected. By filtering the electrical signal, the DC component may be easily removed leaving only the desired difference frequency. Note however that the time dependent phase term is still present. Consequently, if nothing is done to lock these frequency variations, the resulting RF signal may have an unacceptable large bandwidth. A mechanism must be put in place to lock the time dependent phase terms of each signals.

External frequency modulators, such as acousto-optics cells may be used, to up-convert the optical frequency of one arm. This way, only one laser is needed and both phase terms are equal. The major drawback with this approach is that the generated frequency is limited to the bandwidth of the modulator (approximately 2 GHz for acousto-optics). A second approach would be to use the integrated optics frequency modulator as described in section 2.3.2.2. Another option, is to use a third laser in the system depicted in Fig. 2.11, to act as a master laser on which the phase of the other two lasers would be locked. This method is depicted in Fig. 2.12. The reference laser source, called the "master", is driven by a low frequency microwave signal superimposed to the laser's bias current. This oscillating drive current creates a frequency modulation of the light output. As seen in section 2.1, the optical output signal has several sidebands spaced by the modulating frequency f_m. This is shown in Fig. 2.13. Each sideband, has a linewidth equal to the fundamental mode. The modulated optical signal of the master laser is injected in each "slave laser" which are used as bandpass optical amplifiers for selected sidebands of the master laser. The bias current and temperature of the slave lasers are adjusted so that their respective output frequency matches an harmonic of the master laser (Fig 2.12b). For laser diodes, a one milliamp variation in the bias current corresponds typically to a frequency shift of 3 GHz of the emitted optical signal, and a one degree Celsius variation may result in a 30 GHz shift. The phase jitters of the slave lasers ($\phi_1(t)$, $\phi_2(t)$) will consequently be locked on the phase jitter of the master laser, and cancel out at detection.

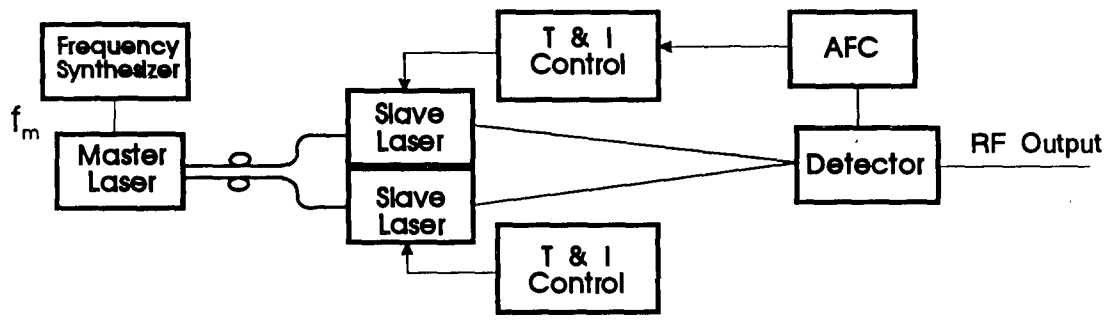

Figure 2.12 Dual slave lasers, controlled by a single master laser, configuration. The slave lasers are current and temperature controlled to lock on different FM harmonics of the master laser.

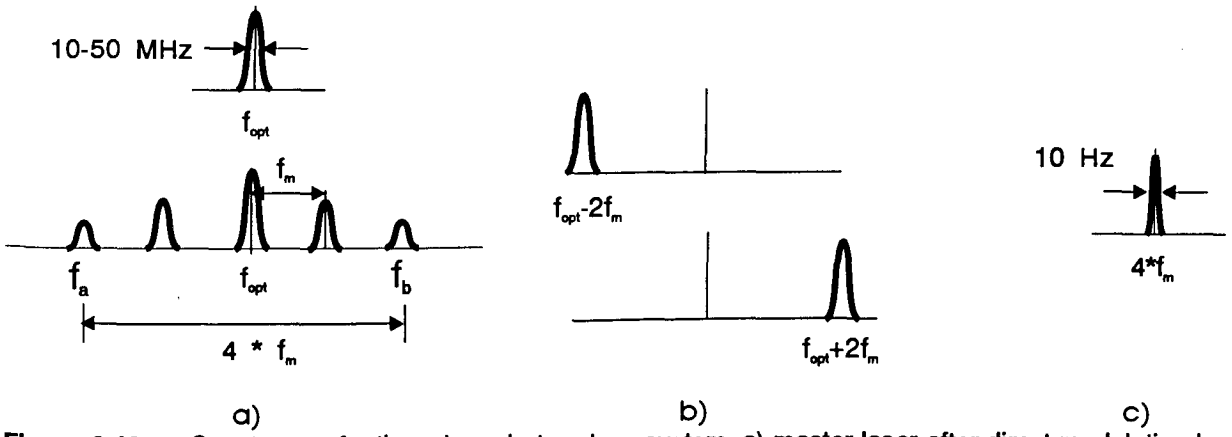

Figure 2.13 Spectrums of a three-laser heterodyne system. a) master laser after direct modulation by a frequency f_m. b) slave lasers tuned to filter specific harmonic. c) beat signal detected

Another approach to heterodyning is to use a single slave laser to provide both frequencies. Fig. 2.14 shows this approach. Multi-mode laser emits on many frequencies, defined by the simple relation:

$$\Delta f = \frac{c}{2nL} \tag{2.15}$$

where c is the speed of light, n is the refractive index of the lasing material and L the cavity length. By proper selection of the parameters, Δf could be made equal to the desired microwave frequency. Typical laser diode cavities are in the range of 250 to 1200 μm which corresponds to a frequency range of 35 to 170 GHz.

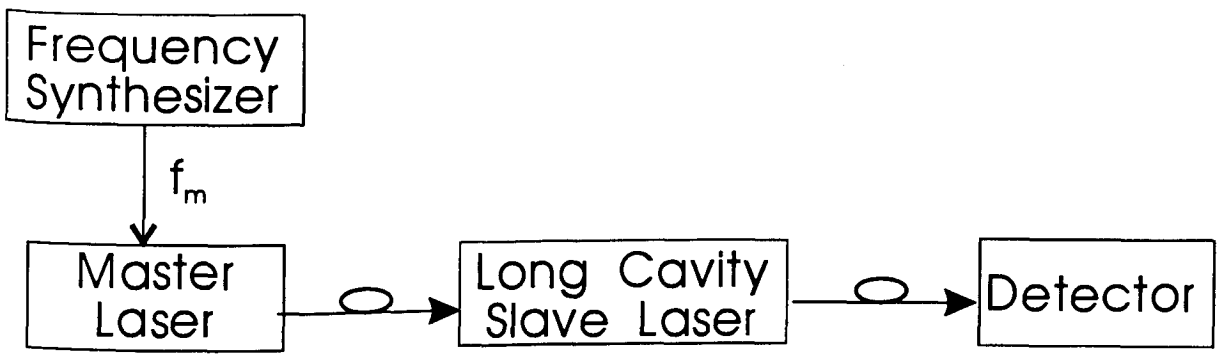

Figure 2.14 Single long cavity slave laser, controlled by a master laser. Two modes of the multi-mode slave are excited from the harmonics of the master output beam.

Fig. 2.15 shows an example of the microwave spectrum generated by this method [2.26]. A 35 GHz beat signal was generated from a 1.2 mm long cavity slave laser. The slave laser was injection locked on the ±3 sidebands of a master laser which was directly modulated with a 5.846 GHz signal. A 3dB spectral width of 6 Hz was achieved.

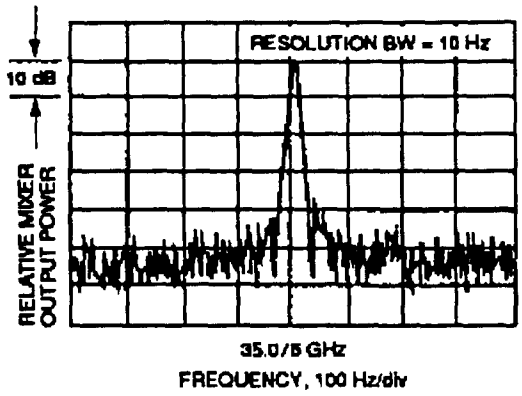

Figure 2.15 Microwave spectrum of the generated signal of from a setup similar to Fig. 2.13 [2.26].

One drawback with this approach is that the generated RF frequency depends on the laser cavity length. One the laser has been cut, the RF frequency is set. For a static frequency, this approach may be attractive since it requires only two lasers. If multiple frequencies are required, the three-laser approach is to be preferred.

3.0 OPTICS-to-RF CONVERSION

At the antenna, the information residing on the optical carrier must be converted back to the electrical domain for radiation into open space, by each element. Moreover, to allow for beam steering, phase and amplitude of the microwave signal must be conserved. In this chapter, potential detectors are reviewed.

A number of devices can be used for optics-to-RF conversion. The most common ones are:

a. PIN photodiodes,
b. Schottky-barrier diodes,
c. APD photodiodes,
d. Field Effect Transistors (FET).

Those devices must meet very high performance requirements. The conversion efficiency needs to be very high with a minimum of added noise since the received optical signal power will most often be very weak. The detector must be sensitive to the selected optical wavelength. The bandwidth, or the response time, of the detectors must also be considered since detection of signals modulated in the GHz range is required. Compatibility, or integration complexity, with the rest of the antenna circuitry is also an important factor.

Each of the stated detector types presents some interesting properties. For example, PIN and Schottky diodes allow conversion of high frequency signals, the avalanche photodiodes (APD) provide internal gain for amplification of small signals, and the FETs, because of their fabrication process, permit excellent integration capabilities.

In this section, each of the above detectors is analyzed. Topics such as efficiency, response time, integrability, noise figures will be covered.

3.1 PIN PHOTODIODES

A PIN photodiode consists of two semiconductor regions doped with opposite polarities, separated by an intrinsic region. Fig. 3.1 shows a schematic representation of a PIN. If the energy of the photons incident on the diode is equal to or higher than the semiconductor bandgap energy, electron-hole pairs will be created in the depletion region. In semiconductor material, the conversion efficiency of photons to electron-hole may be approximated by the exponential law: [3.1]

$$\eta = (1-R)\left[1-\frac{e^{-\alpha W}}{(1+\alpha L_p)}\right] \qquad (3\text{-}1)$$

where R is the reflectivity of the incident surface, α the absorption coefficient of the material, and W its thickness and L_p the diffusion length. In practice R can be made very small by the use of antireflection coatings. The absorption coefficient, α, is strongly wavelength dependent, as shown in Fig. 3.2. The GaAs technology is sensitive to wavelengths from 0.6 μm to 0.88 μm. For longer wavelengths, 1.3 - 1.5 μm, InGaAsP and InGaAs must be used. For shorter wavelengths, Si is a better candidate.

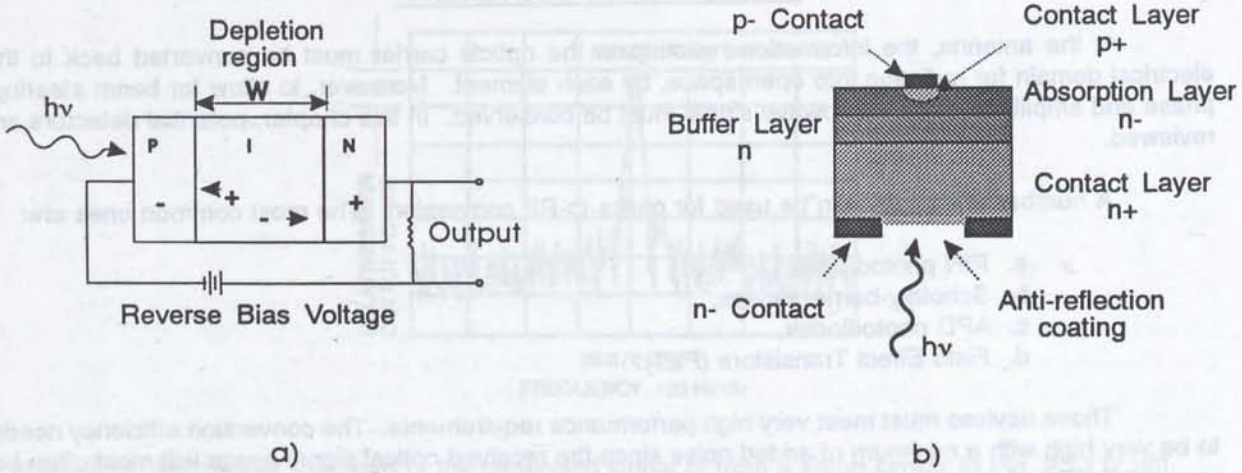

Figure 3.1 Schematic view of a PIN photodetector a)Principle of operation b) practical structure.

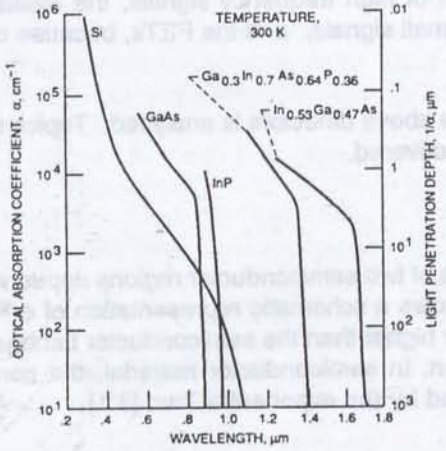

Figure 3.2 Absorption coefficient as a function of wavelength for various materials.

Assuming a GaAs PIN diode made with a 3 μm thick absorption region, a conversion efficiency close to 95% could be attained if the illumination is done with an 800 nm wavelength signal ($\alpha = 10^4$ cm^{-1}). Similar results could be obtained with other combinations of detection material and wavelengths.

Typical bandwidths of high performance PIN diodes may reach 25 GHz [3.2], some have been shown to reach 50 GHz [3.3] and 67 GHz [3.4]. The frequency response of a PIN diode is limited mainly by two factors; the time it takes the carrier to drift across the depletion region and the RC time constant of the device and external circuit. A narrower depletion region would reduce the transit time but would also reduce the quantum efficiency. Moreover, a small active area makes it difficult for fabrication as well as for light injection as shown in Table 3.1.

PIN diodes present however, an important drawback. Their vertical structure renders them incompatible with the field effect transistor (FET) which has a horizontal structure. Integration of the two devices is consequently very difficult. This is of little importance if the complete receiver circuit is made only of PIN diodes but if a mixture of technologies is required, special consideration for the integration will need to be taken. Planar photodetectors are then needed.

Table 3.1 gives some characteristics of a number of commercially available PIN diodes.

Table 3.1 Characteristics of a number of commercially available high speed PIN diodes

Manufacturer	Model	Material	Optimum Wavelength (nm)	Active Area (μm^2)	Bandwidth (GHz) 3dB point	Peak Responsivity (A/W)
Opto-Electronics	PD-15	Si	850	5600	8.0	0.2
Antel	AR-S3	Si	850	3600	14	0.28
Antel	AR-D28	InGaAs	1550	2000	15	0.4

3.2 SCHOTTKY-BARRIER PHOTODIODES

Schottky-barrier photodiodes are somewhat similar to PIN diode except that in the Schottky diodes, the p^+ region has been replaced with a metal to semiconductor interface (Schottky contact). Higher frequency bandwidth is possible. A cross section view of a typical Schottky-barrier photodiode is shown in Fig. 3.3. It consists of thin semitransparent metal film of a few tens of nanometres mounted on an epilayer which in turn is grown on a substrate.

Typical quantum efficiencies of Schottky-barrier diodes are in the order of 30%. This rather low efficiency is mainly due to the poor transmissivity of the semi-transparent Schottky contacts. The most commonly used metal for these contacts are Au, Al which have poor transmissivity. For example, gold contacts have a transmittance of only 55% for a 0.85 μm wavelength. To increase the efficiency, a number of techniques have been suggested. In [3.5], the gold contact pads were replaced with an alloy of indium tin oxide (ITO) which has a transmittance close to 93% in the wavelength region of 0.4 μm to 0.9 μm. An efficiency of 60%, at 830 nm, was reported. Anti-reflection coatings, on top of the semi-transparent Schottky barrier, was shown to increase the quantum efficiency to 40% at 0.83 μm and up to 70% at 0.633μm [3.6].

Very high detection bandwidth are possible with this kind of detectors. Commercially available devices have attained bandwidth up to 60 GHz [3.7]. Laboratory prototypes have been reported with bandwidth of up to 110 GHz. [3.8],[3.9]

Most of the Schottky-barrier photodiodes are based on GaAs technology which render them sensitive to wavelengths in the 0.8 μm region. For applications in the 1.3 to 1.5 μm, Schottky contacts on p-type GaInAs have been demonstrated[3.10], [3.11]. Table 3.2 gives some characteristics of a number of commercially available Schottky diodes.

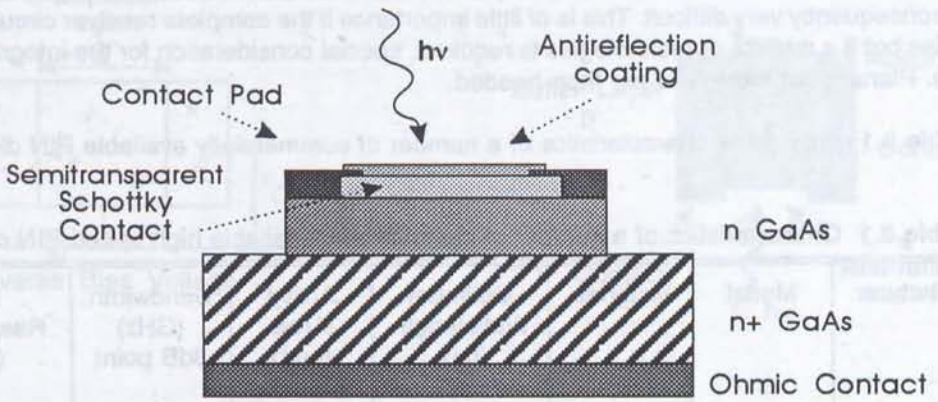

Figure 3.3 Cross section of a Schottky-barrier photodiode.

Table 3.2 Characteristics of a number of commercially available Schottky photodiodes.

Manufacturer	Model	Material	Optimum Wavelength (nm)	Active Area (μm^2)	Bandwidth (GHz) 3dB point	Peak Responsivity (A/W)
New Focus	1002	GaAs Schottky	400-900	110	60	0.2
New Focus	1012	InGaAs Schottky	950-1600	110	45	0.4
Hoescht Celanese	Y-35-5252	GaAs / ITO Schottky	840	500	18	0.4

3.3 AVALANCHE PHOTODIODE (APD)

If the intensity of the received optical signal is low, amplification stages may be needed. In many applications however, the noise inserted by a pre-amplifier stage still degrades the performance too much. Improved performance can be obtained by using APDs. Amplification is intrinsically provided inside the APD device, before the signal enters any external electronic amplification stage where it is corrupted by thermal noise.

The gain of the APD is essentially proportional to the reverse voltage applied. Gains between 1 and 10000 are achievable. The thermal noise of an APD is the same as that of a PIN. As a result, even though the multiplication process introduces excess noise, if the dominant noise source was from the preamplifier, the signal-to-noise ratio could be improved. The required bias voltage is relatively high, typically 100 V. However, with an optimum gain, APDs can provide about 15 dB more receiver sensitivity than that achieved by a PIN diode.

The frequency response of APDs at low multiplication values is essentially the same as for PIN diodes. However, as the gain is increased, the number of electron-hole pairs increases and so does the time required to collect them all. Consequently, the detector response time also increases. Because the response time and the bandwidth are inversely proportional, any increase in the gain is at the expense of the bandwidth. In the case of PIN, the absence of gain results in high bandwidth. A typical bandwidth/gain curve is as shown in Fig. 3.4 [3.12].

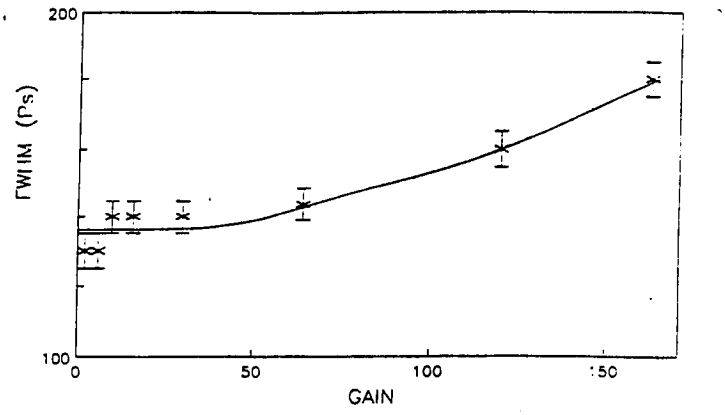

Figure 3.4 Typical APD pulse response versus gain [Ref. 3.12]

3.4 FIELD EFFECT TRANSISTOR (FET)

FETs have several advantages over photodetectors [3.13]. First, the detected signal is internally amplified through the device transconductance. Second, if high electron mobility FETs (HEMTs) are used, an improvement in the output signal-to-noise ratio can be obtained [3.14]. Third, the optical absorption coefficient and the energy band gap of the material used for HEMTs, (GaAlAs, InGaAs, InGaAsP) can be tailored to optimize the performance for specific optical wavelengths. Fourth, integration of the optoelectronic device (the FET) on a single chip with other microwave components also requiring FETs would be simpler. Frequency response of HEMT's have been reported in the 60 and 90 GHz [3.14-3.15].

The fundamental photodetection mechanism in a FET is similar to the other types of detectors mentioned above. Under illumination, electron-holes pairs are created if the incident photons energy is greater or equal to the semiconductor bandgap. These electron-hole pairs are then collected by the gate and drain to contribute to the photocurrent. Thus, illuminating the gate region has the same effect as reducing the reverse bias. A number of excellent review papers on the optical control of FETs have been published [3.16- 3.19].

One drawback with FET is the optical loss that occurs due to the coverage by the gate and drain contacts. Fig. 3.5 shows a typical illumination mechanism of the FET. Optical energy is lost due to this blockage. Coupling efficiency may be as low as 5%. One solution to this problem is to bring the optical signal from underneath. However, this requires some special fabrication technique with material transparent to the wavelength.

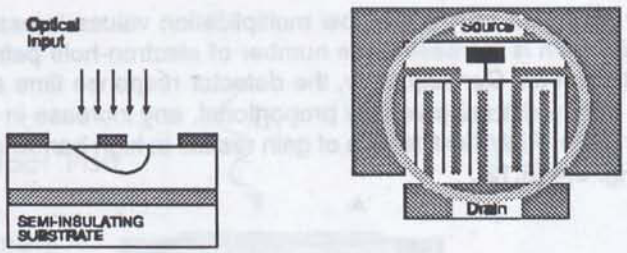

Figure 3.5 Typical illumination mechanism of a FET.

In [3.20], an AlGaAs laser diode with fiber pigtail was used to illuminate the surface of a GaAs FET. The laser was directly modulated from 300 kHz to 3 GHz. The FET drain-source finger spacing was 3 μm and the device had an electrical frequency response with positive gain up to approximately 30 GHz. Fig. 3.6 shows the optical frequency response of the FET. At 0 dB gain, the optical-to-electrical conversion efficiency of the FET was measured to be 1A/W. It is seen, on Fig. 3.6, that the FET offers a high output gain for low optical modulation frequency but that the gain rolls-off rather quickly. This is explained by various detection mechanism in the FET, one with high gain but narrow frequency bandwidth and a second one with large bandwidth but small gain.

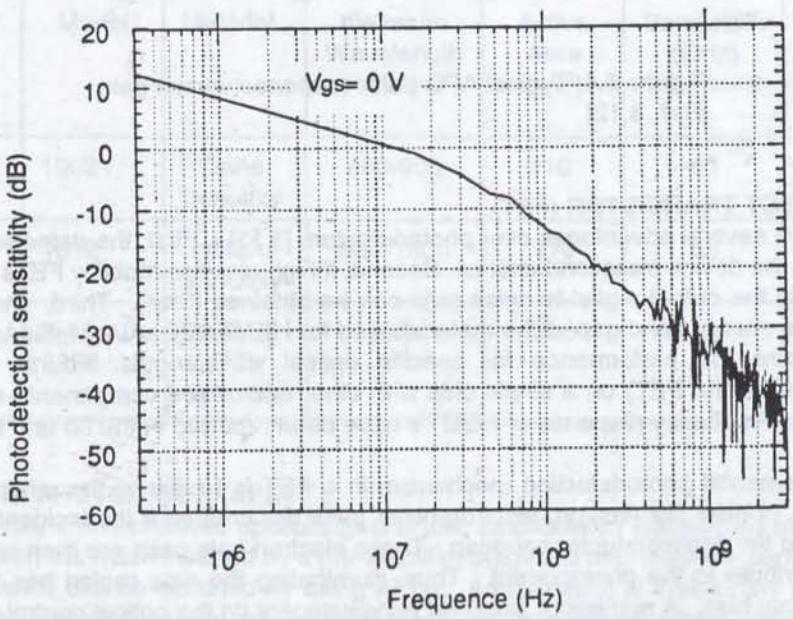

Figure 3.6 Frequency response of an HEMT NE212 for V_{gs} = 0V. [3.20]

4.0 BEAM FORMING NETWORK

The beam forming network (BFN) is responsible for the evaluation of the phase and amplitude weights for each antenna element and the application of these weights. It includes both, the signal processing and signal conditioning. The BFN may take several different architectures, depending on the application (MBA vs PA, transmit section vs receive section), or the desired processing complexity (real time calculation of weights, frequency independent weights). Numerous architectures have been proposed [4.1-4.17]. These architectures essentially fall in two major categories:

1- Discrete control element BFN, where the phase and amplitude are adjusted by discrete elements acting either directly on the RF signal or on the optical carrier. In this case, the weights are calculated by an external processor.

2- Optically processed BFN, where Fourier optic techniques are used to provide the appropriate adjustments on the optical signal. In this type of architecture, the weights are optically calculated.

Before proceeding with the description of these methods, a brief overview of the theory behind PA and MBA BFN will be given.

4.1 BEAM FORMING NETWORK THEORY

A number of excellent publications have been written on the subject of array antenna theory and beam forming network [4.18-4.20] This review section is not intended to replace these publications nor to cover the complete subject. This section is written simply to give the reader a general comprehension of the process involved in the beam formation of PA and MBA. For more detailed information, the reader is referred to the referenced material.

This section is divided into four parts, each dealing with a specific concern of the BFN. In the first part, the classical microwave approach to beam steering is presented. The second part gives an overview of the mathematical considerations required for the formation of multiple beams. Part three deals with the problems associated to beam scanning due to large signal bandwidth. Finally, the last part presents an alternative approach to the classical microwave implementation with time delays.

4.1.1 Beam steering

4.1.1.1 Phased array

Fig. 4.1 shows a schematic representation of a typical linear array with a wavefront propagation angle of θ. The phase and amplitude of the output of each element may be controlled, as indicated, by phase shifters and attenuators. The far field radiation pattern Z(s) of the antenna is defined as the Fourier transform of its aperture field distribution. For a linear array, this may be mathematically described by:

$$Z(s) = \int I(x)\, e^{j\Phi(x)}\, e^{-j2\pi sx}\, dx \qquad (4.1)$$

where I(x) and ϕ(x) are the amplitude and phase distribution across the antenna and s is the position variable in the far field.

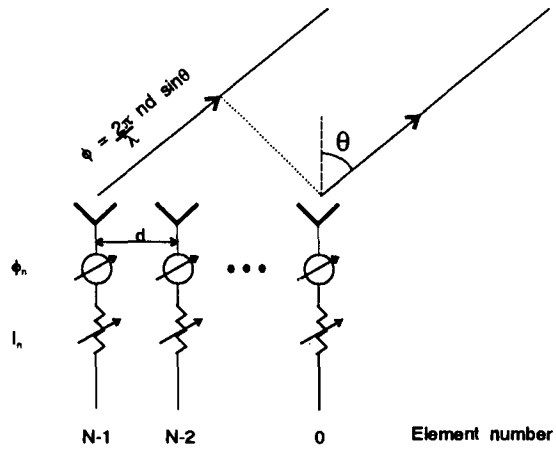

Figure 4.1 Schematic representation of a typical linear array with a wavefront propagation angle of θ.

In a discrete form, Eqn. 4.1 may be rewritten as:

$$Z(\theta) = \frac{1}{N} \sum_{n=0}^{N-1} I_n e^{j\phi_n} e^{-j\frac{2\pi}{\lambda} nd\sin\theta} \qquad (4.2)$$

where θ is the propagation angle, I_n and ϕ_n are the amplitude and phase of the individual elements, λ the transmitted wavelength, and d the spacing between each of the N elements of the array.[1]

Note that strictly speaking another term must be included in the above equations to reflect the radiation pattern of the elements themselves, be it an isotropic pattern or other. If all elements produce a similar radiation pattern, G(θ), the overall wave profile should be expressed as:

$$F(\theta) = G(\theta) * Z(\theta) \qquad (4.3)$$

where * represents the multiplication operation.

To obtain a beam in a certain direction θ_1, i.e. to maximize Z(θ) along θ_1, the terms of Eqn. 4.2 must add in phase for $\theta = \theta_1$. From Eqn 4.2, it is seen that the phase settings ϕ_n must be:

$$\phi_n = \frac{2\pi}{\lambda} nd \sin\theta_1 \qquad (4.4)$$

The phase front, and therefore the radiation pattern, may thus be steered in any direction, by controlling the relative phase ϕ_i between each element of the antenna.

As an example, Fig. 4.2 shows radiation patterns of isotropic radiators, with equal amplitude, spaced by λ/2, with a linear phase variation of 3π/2, and π/2 ($\phi_i = i*\alpha$ with $\alpha = \pi/2, 3\pi/2$), for a twenty-element linear array antenna. From equation 4.4, this correspond to beam directions of ± π/6.

Note however that Eqn. 4.4 assumes a continuous control over ϕ_n. In most systems, ϕ_n will only take a limited number of discrete values, thus creating a distortion of the beam. The resolution, or the smallest increment Δφ required, will depend on a number of factors such as the number of antenna elements, the steering angle, the power loss acceptable, etc.

---

[1] In two dimensions:

$$Z(\theta_x,\theta_y) = \sum_n \sum_m |I_{m,n}| e^{j\phi_{m,n}} e^{-j\frac{2\pi d}{\lambda}[m\sin\theta_x + n\sin\theta_y]}$$

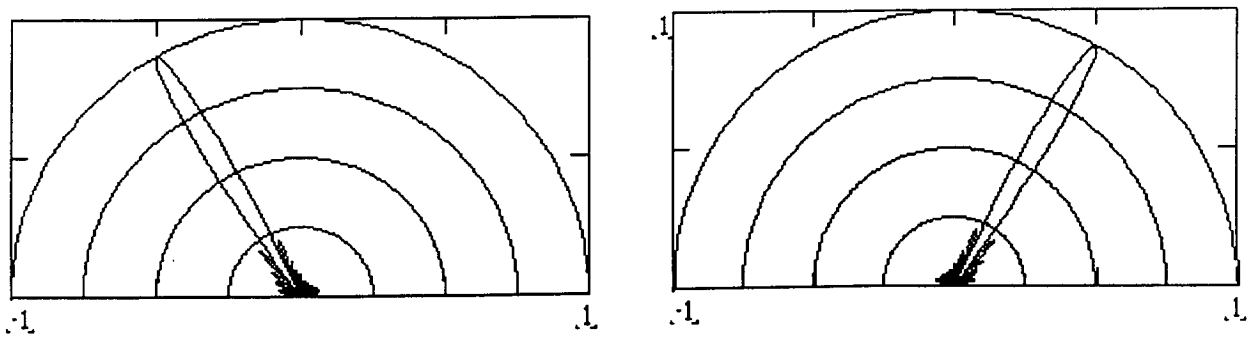

Figure 4.2 Normalized radiation pattern of a 20 isotropic element linear array with equal amplitude spaced by $\lambda/2$ with a linear phase variation of a) $3\pi/2$ and b) $\pi/2$.

4.1.1.2 Multiple beam antenna

In MBA, the Fourier transform is accomplished by the antenna dish rather than by far field propagation as in PA. Beam steering in MBAs becomes somewhat easier since to each horn is associated a specific footprint in the far field region as seen in Fig. 1.5. Therefore, in most cases, MBA beam steering is a matter of selecting the proper horn. All that is required is then beam switching. In some cases however, contoured footprints may be desired. In these cases, many beams are associated, with proper phase and amplitude weights, so as to produce the appropriate footprint.

It will be sufficient for this report to know that MBAs require beam switching, on top of the phase and amplitude control required in PAs. The interested reader may consult the reference material to learn more about the mathematics behind the phase and amplitude control of MBAs.

4.1.2 RF Bandwidth Criteria

The above mathematical description for PAs considered that the emitted frequency was single tone. In many applications, however, broadband signals need to be transmitted. For example, in radar applications, very narrow pulses (τ) need to be emitted. This may result in a very large equivalent instantaneous bandwidth ($\Delta f = 1/\tau$). In frequency agile communications systems, the transmitted frequency, even though narrow band, may be hopped over a range of a few GHz.

From Fig. 4.2 and Eqn. 4.2, it is seen that a linear phase slope across the array is needed to produce a beam in a direction θ_1, and that the required phase at the i^{th} element is: $\phi_i = i*(2\pi/\lambda)d\sin\theta_1$ (radians) with respect to the first element. Rewriting this in the form of:

$$\sin\theta_1 = \frac{I\,\phi_I\,\lambda}{2\,\pi\,d} \qquad (4.5)$$

it becomes apparent that if ϕ_i and d stay fix, then a change in wavelength (or RF frequency) will produce a proportional change in the beam angle. It can be shown that the change in the beam angle is given by:

$$\Delta\theta_1 = -\left(\frac{\Delta f}{f}\right)\tan\theta_1 \qquad (4.6)$$

where $\Delta f/f$ is the fractional bandwidth.

The following are worth noting:

a) The aperture size and beamwidth have no effect on the change in beam angle.

b) The amount of variation in the scan angle is dependant on the original beam angle and the effect is most noticeable at large steering angles ($\theta \rightarrow 90$). It is therefore evident that before a bandwidth criteria is specified, the maximum steering angle must be specified.

c) As the frequency increases, the scan angle will decrease.

Fig. 4.3 gives a plot of the signal loss as a function of the normalized frequency shift ($\Delta f/f$) for a linear array (having a 3 dB beamwidth of 0.5°) for two different steering angles of 10° and 4°.

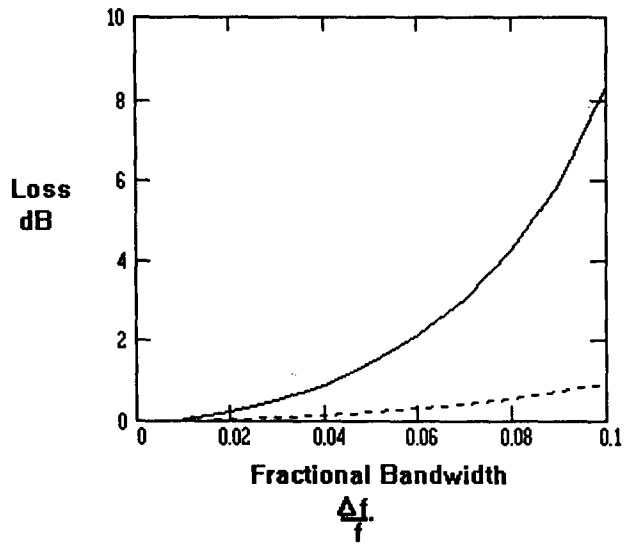

Figure 4.3 Signal loss at transmission angles of 10° and 4°, for a linear PA with a 3 dB beamwidth of 0.5° , due to a transmitted frequency shift of up to 10%, .

Fig. 4.4 shows the signal loss when a similar antenna is used but as a function of the steering angle for frequency shifts of 1% and 5% of centre frequency.

The major problem associated with scanning of the beam, as presented by the above analysis is due to the fact that the phase adjustment is directly related to the frequency of the transmitted signal (Eqn. 4.4). Another approach to provide the steering of the beam, for wideband applications, is by using time delays. The next section will cover this topic in greater detail.

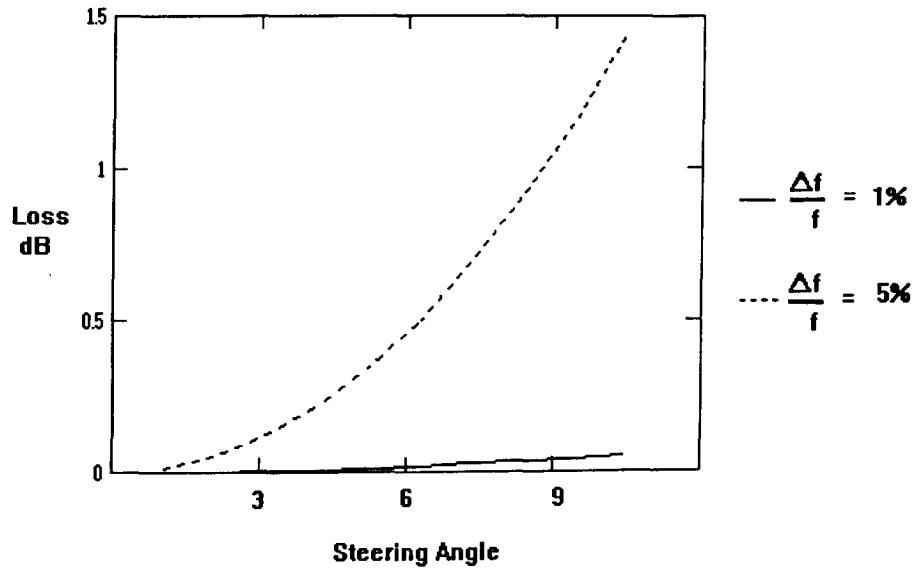

Figure 4.4 Signal loss, at transmission angles from 0 to 10°, due to frequency shift of 1% and 5%, for a linear array having a 3 dB beamwidth of 0.5° (100 elements spaced by λ/2) .

4.1.3 Time Delay

Another way of picturing the interference process occurring at the output of an array, is in terms of time delays, rather than phase shifts. As shown in Fig. 4.5, if the output beam propagates in a direction θ_1 from the array plane, the signal emitted from the last element will need to travel (N-1)*d*sinθ_1 further than the signal from the first element. To have the signals in phase along the propagation plane, the signal emitted from the first element must consequently be time delayed with respect to the signal from the last one by $\Delta t = (N-1)*d/c \sin\theta_1$, where c is the velocity of the emitted RF signal. A criteria for the time delay associated to each element may then be established. For the i^{th} element, the time delay is:

$$t_i = \frac{i*d}{c}\sin\theta_1 \qquad (4.7)$$

The beam steering then becomes independent of the RF frequency. The frequency dependant phase shifts have been replaced with time delays which depends only on the antenna size and element spacing.

Rewriting Eqn 4.2, and including the frequency term, the far field pattern may be expressed as:

$$Z(f_c,\theta) = \sum_{n=0}^{N-1} e^{j\left(2\pi f_c(t-\tau)-\frac{2\pi}{\lambda}\, d\sin\theta\right)} \qquad (4.8)$$

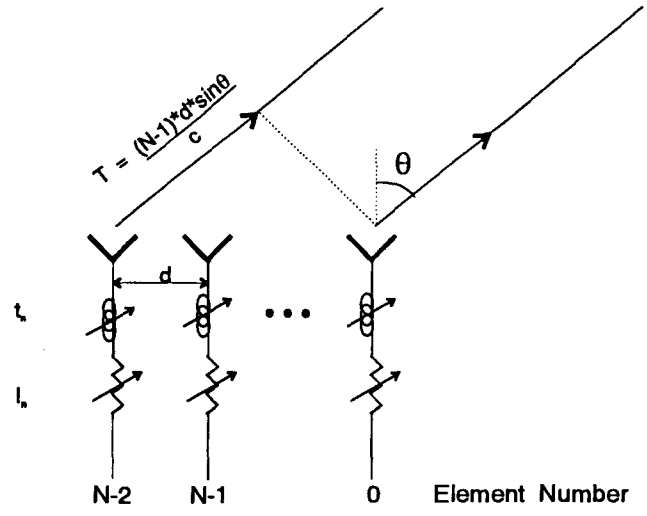

Figure 4.5 Time delay steerable linear phased array.

For example, suppose a 20 GHz signal to be steered at angles θ from 0° to 10°, from a PA antenna whose 100 elements are spaced by λ/2. Suppose also that the steering resolution should be such that a maximum intensity loss of 0.5 dB in the signal strength be experienced.

The largest steering angle will dictate the largest time delay.

$$\Delta t_{max} = (N-1)*\frac{d}{C}\sin\theta = \frac{99*\frac{\lambda}{2}}{c}*sin10^{\circ} = \frac{49.5}{20*10^{9}}*sin10^{\circ} = 0.43\ nsec$$

The maximum time delay would then be 0.43 ns.

The minimum steering angle is found from the resolution criteria. For the antenna considered, the beam scanning must be smaller than 0.2° to suffer from a signal loss no larger than 0.5 dB. Consequently, the minimum time delay is measured to be:

$$\Delta t_{min} = \frac{d}{C}\sin\theta = \frac{\lambda}{2c}*sin0.2^{\circ} = \frac{1}{40*10^{9}} * sin0.2^{\circ} = 8.7 * 10^{-14}\ sec$$

In the rest of this chapter, different BFN implementation, using both conventional phase shifters and true time delays will be described.

4.2 DISCRETE COMPONENTS

In this section, a number of architectures that use discrete components to implement the BFN will be analysed. As seen in the previous section, these components may operate either on the phase of the RF or optical signal or on the time delay. It must be realized that the architecture presented will in no way cover all possibilities. They are presented solely to give the reader an overview of various implementation possibilities. Each application will require a detailed system analysis to find the best architecture. The selected architecture for a particular application may even contain a mix of technolgies presented here.

4.2.1 Conventional RF Phase Shifters

This implementation is similar to a conventional microwave approach where the phase shifts and amplitude controls are done directly on the RF signal. In this case, the optics serves only as a mean to distribute the RF signal to the many antenna elements via optical fiber. Fig. 4.6 shows a typical implementation of such a system. The RF signal is converted on the optical carrier using one of the techniques discussed in chapter 2 (direct modulation, external modulator or heterodyne). After distribution to each element, the modulated optical signal is converted to an electrical signal using either a photodetector or by direct conversion on the radiating element (chapter 3). Once the RF signal is converted into an electrical signal, conventional phase shifters and attenuators are used to create the proper shifts.

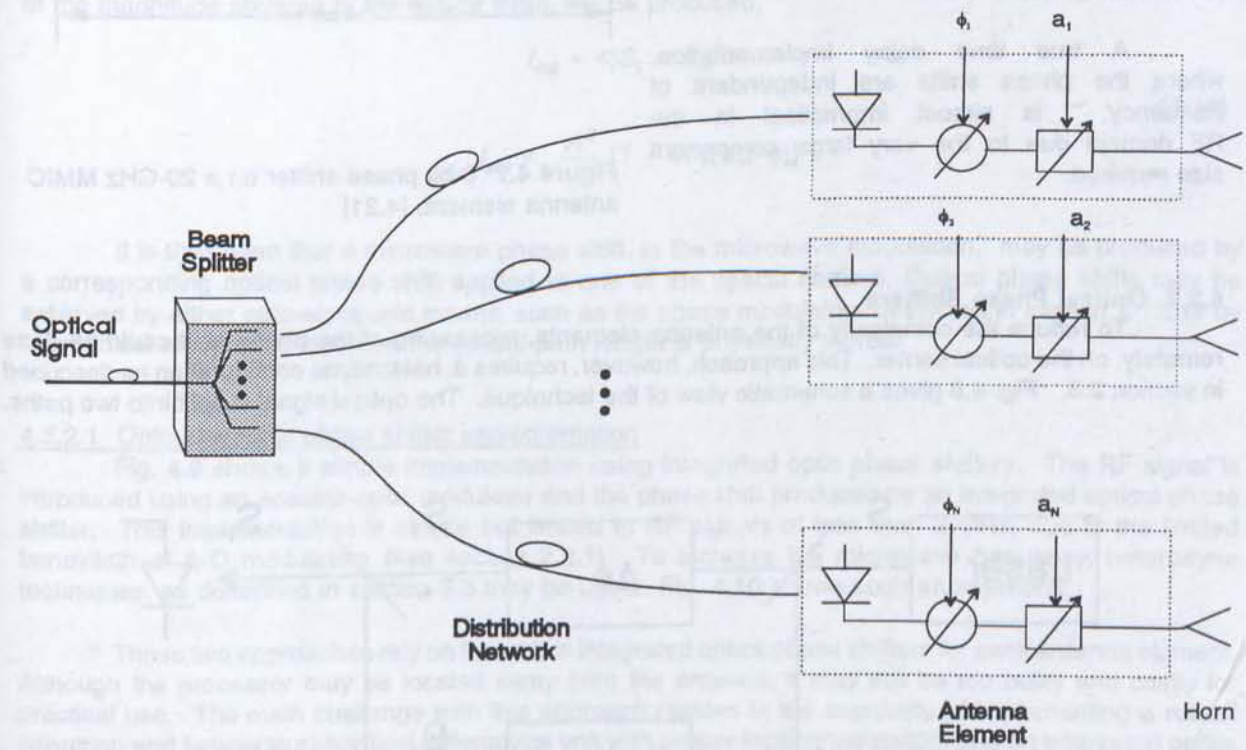

Figure 4.6 Schematic representation of a PA antenna, with optical signal distribution but electronically controlled.

The main advantage of this approach resides in its very high circuit integration capability. With today's technology, RF phase shifters may be implemented directly using a microwave monolithic integrated circuit (MMIC). Fig. 4.7 shows an 3-bit phase shifter on a 20-GHz radiative element giving 8 different phase shifts [4.21]. MMIC phase shifters are usually implemented via "time delays". The path length of the RF signal is varied to produce the appropriate phase shift.

This approach, however, becomes cumbersome for large phased array. Typically 1 or 2 electrical control lines are required per bit. For example a 1,000 element PA using 6-bit phase shifters will require 6,000 to 12,000 control lines. Another drawback with this approach is the bandwidth limitation due to the use of phase shifters as discussed in section 4.1.3. A 100-element antenna, transmitting a 20GHz signal with a 1GHz bandwidth would suffer a 1.4 dB loss for frequencies at the end of the bandwidth when the beam is steered at an angle of ±10° with respect to the plane normal to the antenna, and a 9 dB loss if the same beam is steered at ±90°.

A true time delay implementation, where the phase shifts are independant of frequency, is almost impractical in the RF domain due to the very large component size required.

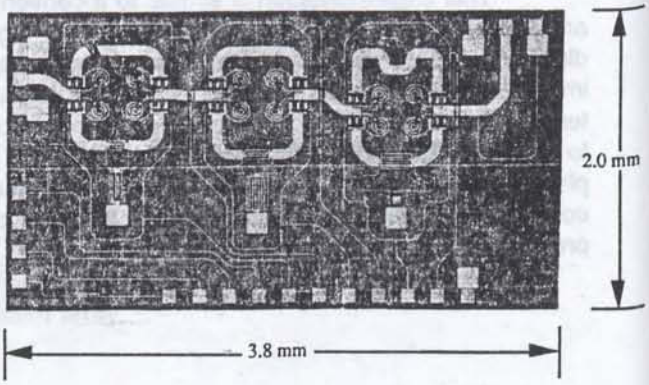

Figure 4.7 3-bit phase shifter on a 20-GHz MMIC antenna element. [4.21]

4.2.2 Optical Phase Shifters

To reduce the complexity of the antenna elements, processing of the phase shift could be done remotely, on the optical carrier. This approach, however, requires a heterodyne configuration as described in section 2.3. Fig. 4.8 gives a schematic view of the technique. The optical signal is split into two paths.

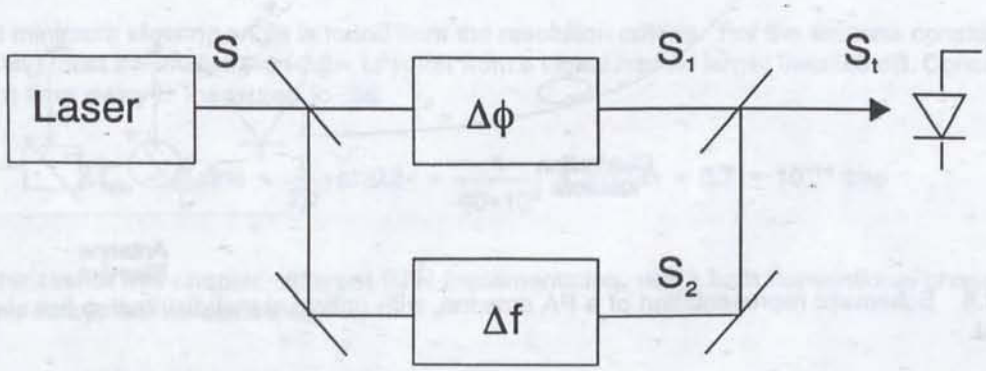

Figure 4.8 Schematic representation of an optical phase shift implementation. In one arm the optical signal frequency shifted while a phase shift is introduced in the other arm.

The signal in one path is frequency shifted by the desired RF frequency while the optical signal in the other path is phase shifted. The mathematics may be expressed as follow.

Giving the optical output signal of the laser by,

$$S(t) = A\cos(w_0 t) \tag{4.11}$$

the frequency shifted version becomes,

$$S_1(t) = \frac{A}{2}\cos((w_0+w_r)t) \tag{4.12}$$

and the phase shifted version,

$$S_2(t) = \frac{A}{2}\cos(w_0 t + \phi) \tag{4.13}$$

By mixing those two optical signals on the detector, an electric signal, equal to the time average of the magnitude squared of the optical input, will be produced,

$$I_{out} = \langle |S_1 + S_2|^2 \rangle$$

$$I_{out} = \frac{A^2}{4}[1 - \cos(w_r t - \phi)] \tag{4.14}$$

It is thus seen that a microwave phase shift, in the microwave modulation, may be produced by a corresponding optical phase shift applied to one of the optical carriers. Optical phase shifts may be achieved by either opto-electronic means, such as the phase modulators described in section 2.1.2 or by mechanical movement, whereby the optical path length is physically varied.

4.2.2.1 Opto-electronic phase shifter implementation

Fig. 4.9 shows a simple implementation using integrated optic phase shifters. The RF signal is introduced using an acousto-optic modulator and the phase shift produced by an integrated optical phase shifter. This implementation is simple but limited to RF signals of less than 2 GHz, due to the limited bandwidth of A-O modulators (see section 2.2.1). To increase the microwave frequency, heterodyne techniques, as described in section 2.3 may be used. Fig. 4.10 shows such an approach.

Those two approaches rely on the use of integrated optics phase shifters for each antenna element. Although the processor may be located away from the antenna, it may still be too bulky and costly for practical use. The main challenge with this approach resides in the capability of implementing a robust (vibration and temperature) optical heterodyne unit with proper locking bandwidth and an integrated optics version of the phase and amplitude modulator with low optical loss and required setting accuracy.

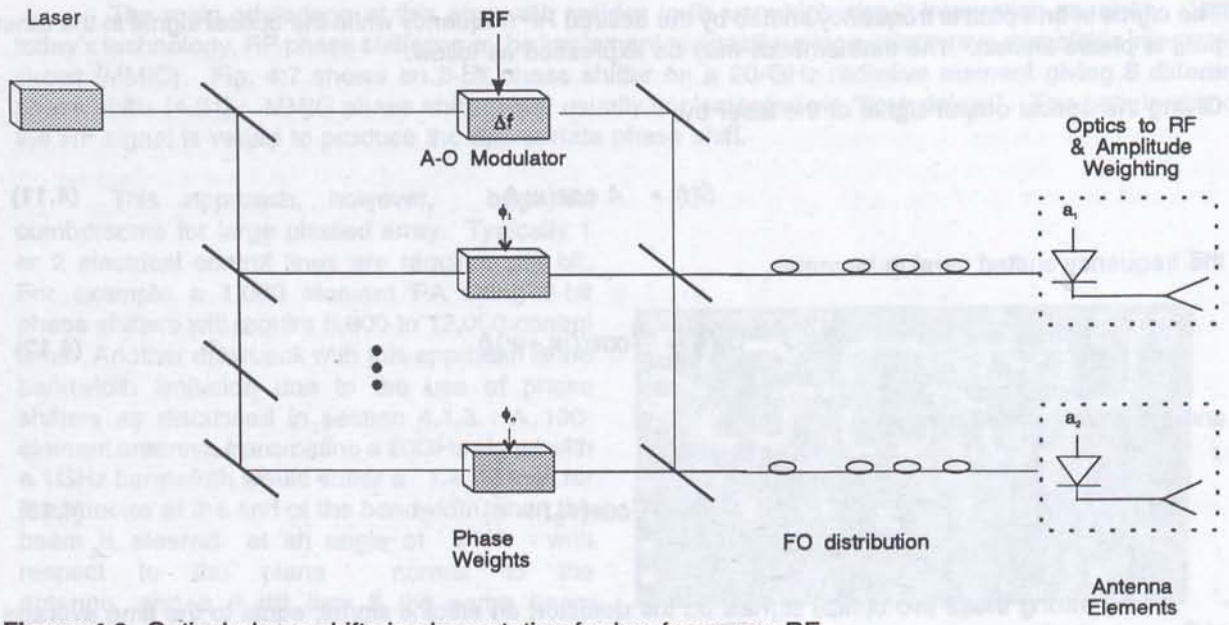

Figure 4.9 Optical phase shifts implementation for low frequency RF

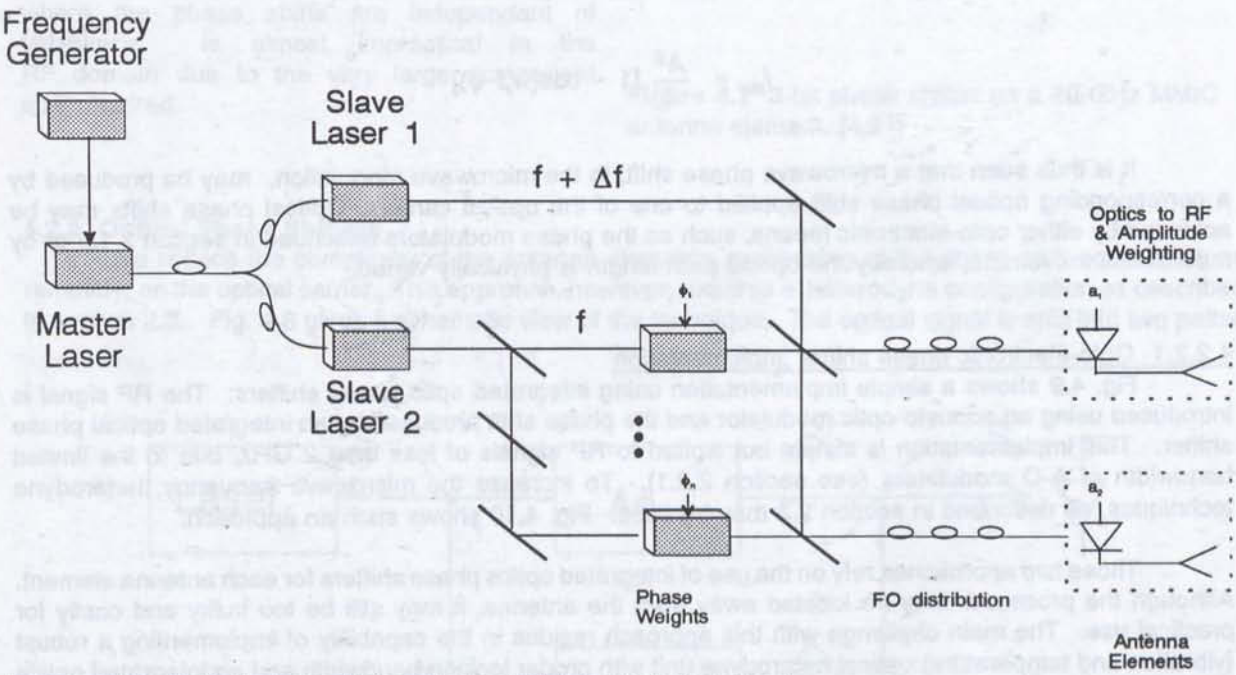

Figure 4.10 Optical phase shift implementation for high frequency

4.2.2.2 Mechanical phase shifters implementation

Mechanical phase shifters, such as deformable mirrors, may be used as an alternative to create the optical phase shift. Fig. 4.11 shows a possible implementation. As in the previous implementation, the optical signal is split into two paths, one giving the frequency reference and the other one being used to

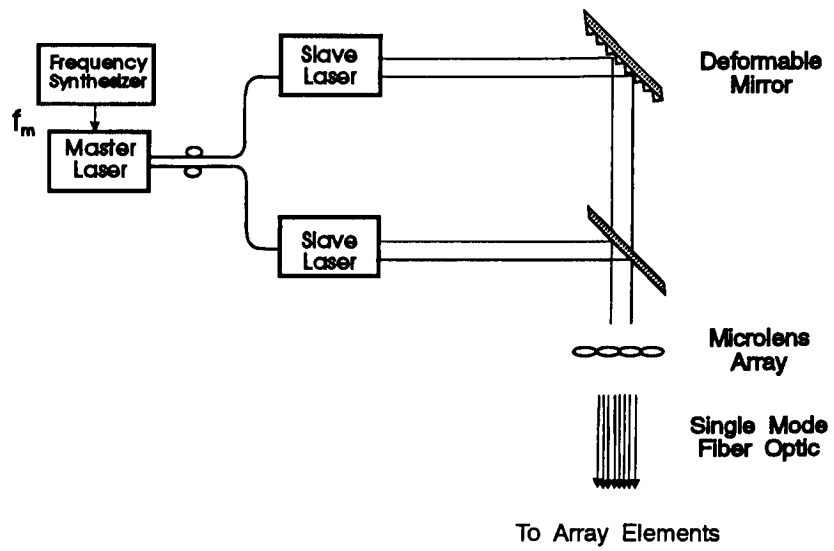

Figure 4.11 Mechanical optical phase shifters using deformable mirror

provide the phase information. The phase shift is introduced by the deformable mirror which is in fact composed of a multitude of small mirrors mounted on some sort of piston (Fig. 4.12). Each mirror is individually addressable. To create a phase shift, the mirror is retracted from its original position. Since to each mirror may be associated an antenna element, the phase weights may be applied by properly setting the position of the corresponding mirror. Since in an heterodyne structure, optical phase shifts directly translate to microwave phase shift, mirror movement on the order of a few microns will be , sufficient to introduce phase shift of 0 to 2π on the microwave signal.

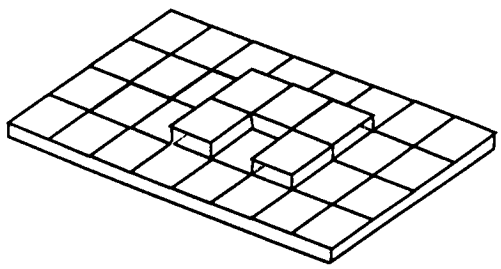

Figure 4.12 Schematic representation of a deformable mirror device. Each mirror element of the device can be translated to different positions.

There are a number of ways to implement these deformable mirrors. The simplest approach is to mount each mirror on a piezoelectric transducer [4.22]. By applying a voltage to the transducer, an expansion of the transducer will result in a displacement of the mirror. The disadvantage of this method is the integration difficulty for large arrays. Each transducer must be independently cut, electrical wired solder to it, and a mirror mounted. A three by three mirror matrix has been assembled in our lab. The tranducers measured 3.2 mm x 3.2 mm x 3.2 mm and the matrix was 25 mm x 25mm (Fig. 4.13). Moreover, piezoelectric transducers requires very high voltages (100 to 1000 Volts) to operate.

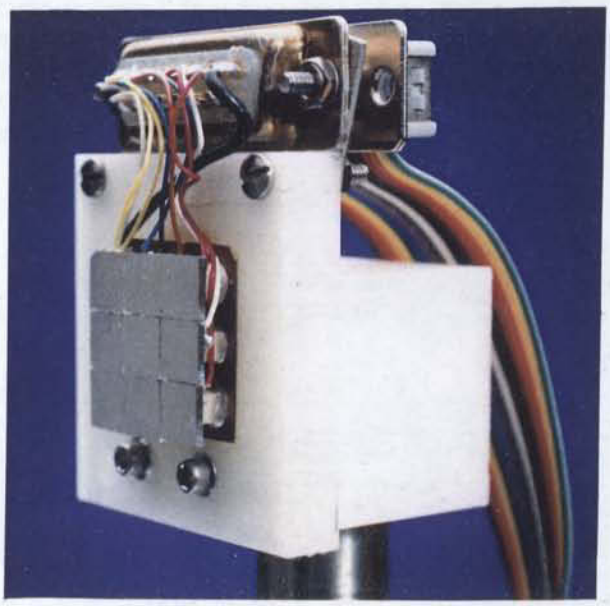

Figure 4.13 Example of a protoype unit of a 3X3 deformable mirror based on piezoelectric transducers.

Another approach is through electro-static fields. [4.23-25]. In this case, the mirror is set to a certain electrical polarity while an electrode placed under the mirror is switched to the opposite polarity. The resulting electrostatic field will force the mirror to retract towards the electrode. This approach may be implemented by micro-machining using electron or ion guns. Electric fields required are in the order of 10 V for a 2π phase shift of the optical signal.

This implementation is extremely attractive since with a small set-up, phase weighting of every antenna element can be done. Moreover, using heterodyne techniques, this method may be applicable to any frequency band, and to any phased array, radar and communications applications.

However, this approach is extremely risky. First, heterodyne operation, with all its complications due to vibration and alignments, is required. Second, even though Texas Instrument, under contract with the US Army, has developed prototypes of the deformable mirrors and that the Alberta Microelectronic Centre and the National Optics Institute have some capabilities to pursue similar research in Canada, the deformable mirror technology is not mature yet. Third, optical coupling in the fibre optics creates a problem. Microlens array are needed to minimize the coupling losses and such a technology is also new. Fourth, this architecture, involving optical phase shifts, puts a heavy requirements on the quality of the optical components. Finally, there is an optical power budget problem in that a very powerful laser is required or many BFN units are required to service different sections of the antenna.

4.2.3 Optical Time Delays

The above BFN implementations are based on phase shifting of the RF signal. As mentioned earlier, as the fractional RF bandwidth and the beam steering angle increases, this approach becomes no longer suitable due to beam scanning. True time delay techniques must then be used. Again, a number of approaches have been suggested for such an implementation [4.10-4.15].

A relatively simple approach to a true time delay implementation using discrete components is shown in Fig. 4.14. The various time delays are provided by a bank of fiber optics of different lengths. A "switch" directs the optical signal in the appropriate fiber to provide the desired time delay. This switch may be based on a number of technologies, of which we may name: mechanical switch (moving fiber, moving beam), liquid crystal switch, electro-optic and holographic switch.

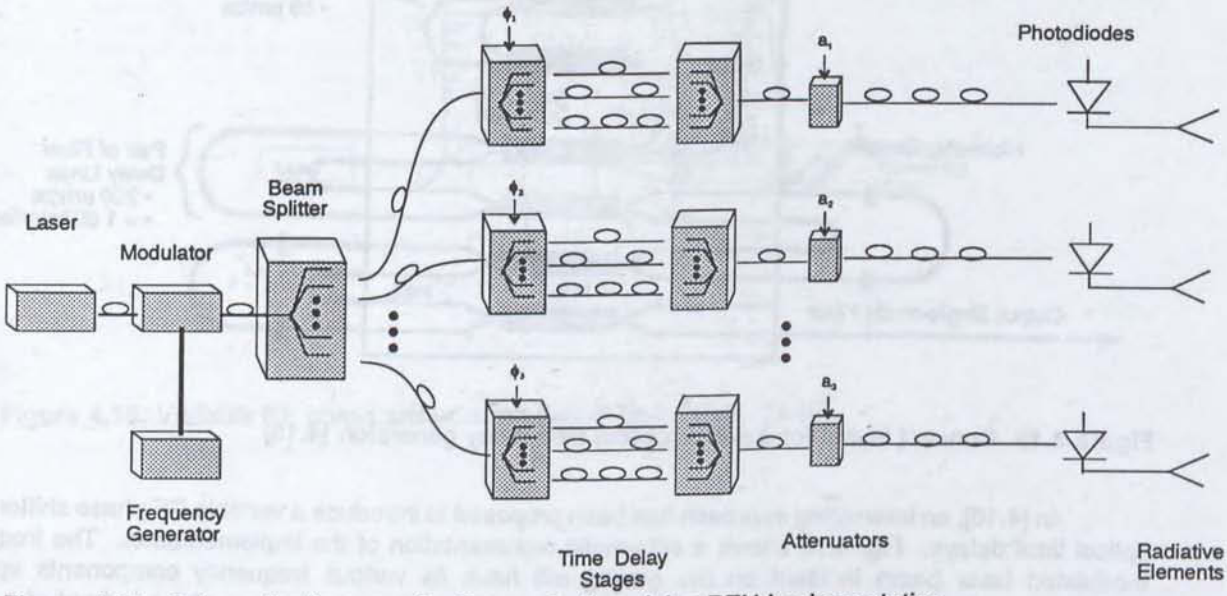

Figure 4.14 Schematic diagram of a fiber optic time delay BFN implementation.

Using the example of section 4.1.4 where a maximum time delay of 0.43 ns was required with a resolution of $8.7 * 10^{-14}$ sec, 4943 fibers would be needed with a variation in length of 17.4 μm (based on a refractive index of 1.5).

One could think of using an electro-optic phase modulator as the time delay unit. As described in chapter 2, by applying an electro-magnetic field to a unixial ferroelectric crystal, the refractive index of the crystal may be modified, consequently changing the propagation velocity inside the modulator and therefore creating a time delay. The mathematics governing this approach is: $\Delta t = \Delta n * L/c$ where Δn is the variation of the crystal (waveguide) refractive index. Using the above example, a variation of the refractive index of 1.14 would be needed if a crystal of 1 cm is used. This is unfortunately impossible with today's technology, but some effort should be pursued to obtain a device, in a waveguide format, which could easily give the proper delays.

The architecture of Fig. 4.14 suggests that the time delays be introduced in parallel, i.e.for each element, the signal is routed in one fiber having the appropriate length. This approach may become cumbersome as the number of elements and the time delay resolution are increased. For a 100-element antenna, requiring a time delay resolution of 10 bits (1024 delays per elements), over 100,000 fibers would be needed. Fig. 4.15 shows a serial time delay unit [4.15]. To each element is associated one device. For a N-bit time delay resolution, there are N branching stations, arranged in series. In each station the light is allowed to follow one of two paths, a short one used as a reference or a longer one introducing the delay. The length of the longer one is doubled at each station. Since, for large arrays the delays may exceed the dimension of an integrated circuit device, fiber optics could be used to provide those long delays. This approach presents some very high insertion loss. It is estimated that a 7-bit delay may show some 20 dB loss [4.15].

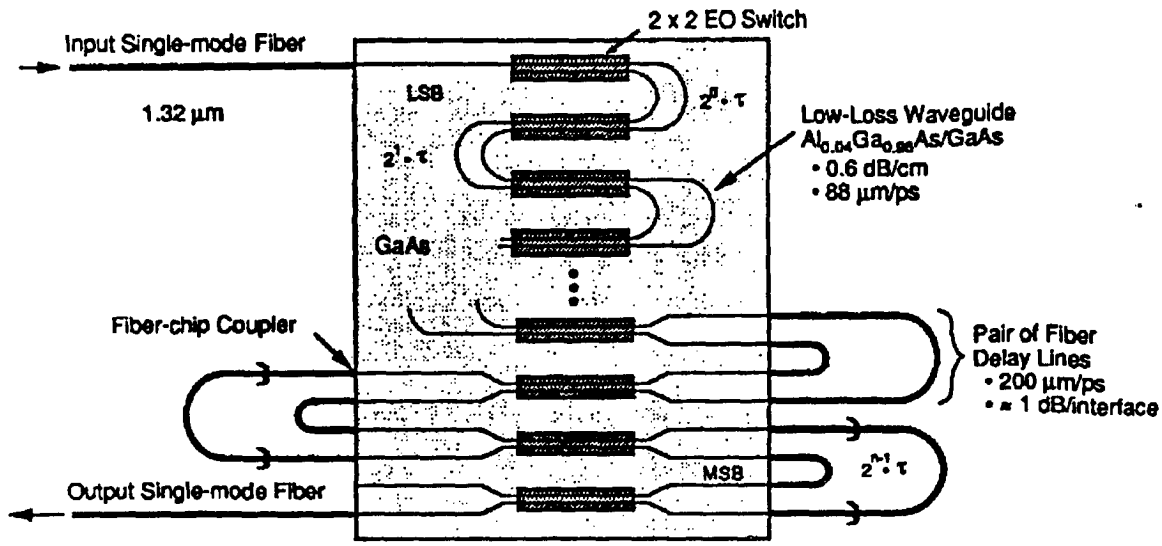

Figure 4.15 Concept layout for a serial optical time delay generator. [4.15]

In [4.10], an interesting approach has been proposed to introduce a variable RF phase shifter using optical time delays. Fig. 4.16 shows a schematic representation of the implementation. The frequency modulated laser beam incident on the grating will have its various frequency components spatially dispersed as shown. These frequency components are imaged on a reference plane in front of a mirror capable of both rotation and translation. It is seen from Fig. 4.16, that each frequency component experiences a different time delay defined by the traveled optical path. This path can be varied by rotation and translation of the mirror. Since the heterodyne process preserves the phase, an RF phase shift equal to the optical phase shift results. This phase shift varies linearly with frequency.

4.2.4 Combination

It is possible to foresee a combination of both discrete electronic RF phase shifters and optical time delays. The combination of both phase shifters and time delays is in fact a known approach, used in conventional RF systems to minimize the problems associated with bandwidth criteria due to the phase shifters and size due to the time delays. In the system proposed here, the time delay part would be done by optical fibers, and would consequently permit the high frequency systems to be implemented without the need of waveguides. A typical implementation structure is shown in Fig. 4.17.

Of course this implementation would present some beam scanning for large bandwidth signals due to the RF phase shifters, although much less than with a complete microwave approach. However, because of the high degree of integration of MMIC components, it could save space when compared to a time delay approach.

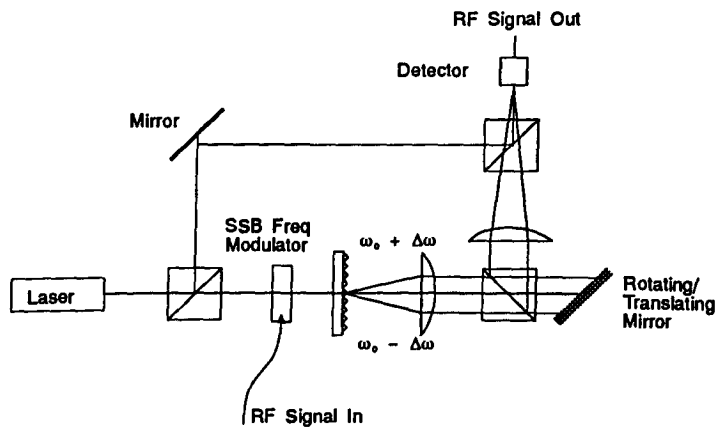

Figure 4.16 Variable RF phase shifter using optical time delay. [4.10].

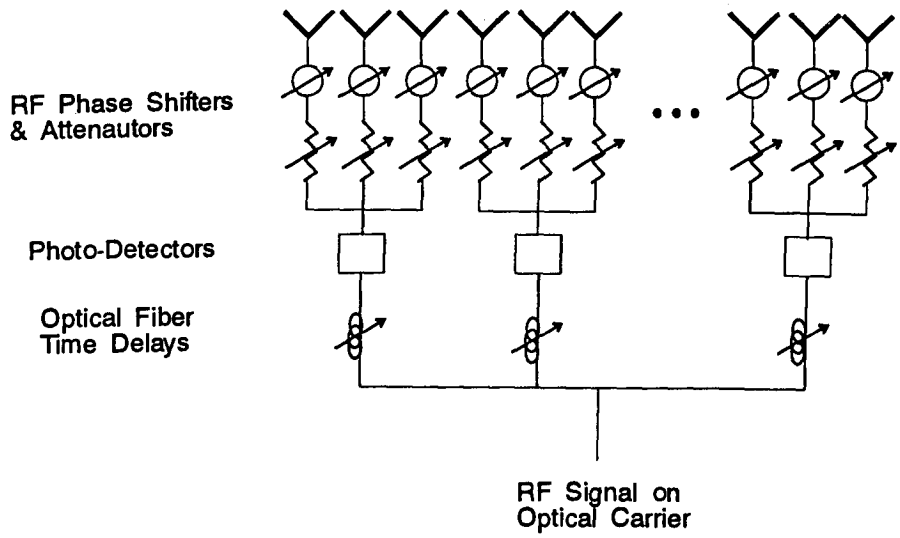

Figure 4.17 Possible implementation structure of a BFN using optical time delays, RF phase shifters and attenuators.

4.3 OPTICALLY PROCESSED BEAM FORMING

The techniques discussed in the previous sections were based on adjusting the phase and amplitude of the signal with some predetermined values. These values were calculated from digital signal processing techniques. As was mentioned in section 4.1, the far field pattern of an array antenna corresponds to the Fourier transform of the antenna illumination. Two dimensional Fourier transform may be rather complex to compute digitally. With an optical processor, a 2-D Fourier transform can be performed in real time by far field diffraction of coherent light.

It can be shown [4.27] that if an object is placed at the focal length of a lens, the relation between the image plane and the object is an exact Fourier transform of the form:

$$U(x_f,y_f) = \int\int_{-\infty} t_0(x_0,y_0)\exp(-j\frac{2\pi}{\lambda f}(x_0x_f + y_0y_f)) \qquad (4.16)$$

where $t_0(x_0,y_0)$ is the transmittance function of the object and

$$x_f = \frac{\alpha}{f} \qquad y_f = \frac{\beta}{f} \qquad (4.17)$$

where α and β are the direction cosines.

If $t_0(x_0,y_0)$ is made to represent the desired far field beam pattern, then on the Fourier plane, the phase and amplitude information is made available. Beam formation is then possible by coherent illumination of a mask representing a scaled down version of the desired beam pattern, and by converting the spatial information of the optical far field into the spectral region in which the antenna emits.

Fig. 4.18 shows the basic implementation as proposed by Koepf [4.28]. The laser beam is split into two paths. In one arm, the frequency information of the RF signal is imposed by mean of an acousto-optic cell or by injection locking of a slave laser. On the other arm, a mask presenting a scaled down version of the far field profile is inserted in the path of the optical signal.

It is then clearly seen that since the optical wave associated to each point on the object plane propagates at a specific angle θ, defined by α and β, each one will travel a different distance to reach a given point on the image plane and consequently relative phase shifts will be introduced. Since photodetectors are square law devices, the phase of the optical signal can only be detected by heterodyne means, by adding another light beam which acts as a frequency reference. By offsetting the frequency of this second beam, the antenna operating frequency and element phase information are then made available. The RF phase shift, ϕ, introduced is defined according to [4.8]:

$$\sin\phi = \frac{(\Lambda\ d\ \sin\theta)}{\lambda\ D} \qquad (4.18)$$

where λ and Λ are the optical and antenna RF operating wavelengths, d and D are the element spacing of the optical detectors on the image plane and of the antenna elements. Beam shaping and beam steering may consequently be formed without computations, simply by modifying the mask at the input of the processor.

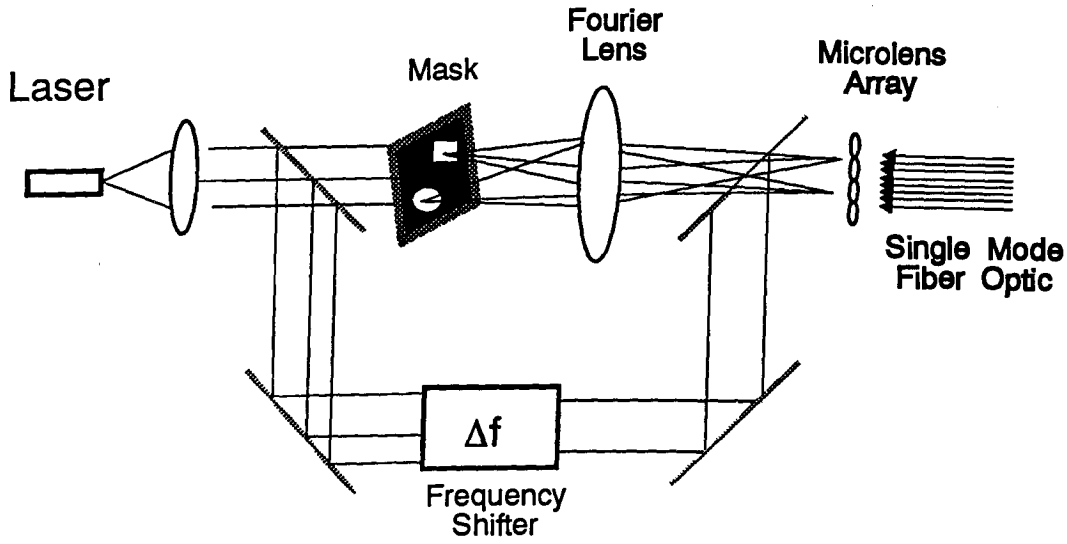

Figure 4.18 Schematic diagram of a generic implementation of a Fourier optic processed BFN

The mask may be a number of different things. For example, in [4.28], Koepf used a simple pinhole which he was moving, to simulate beam steering. In [4.7], the authors used a liquid crystal light valve (LCLV) and in [4.8], a magneto-optic spatial light modulator (SLM). Even though the pinhole approach is simple and allows very high contrast ratio, it is unsuitable for rapid reconfigurability and multiple beams. The approaches using the SLM and the LCLV offer easier reconfigurability but poorer contrast ratios.

4.4 RECEIVED SIGNAL

In the previous sections, the architectures presented showed only the transmit section. In this section, it will be shown that these same architectures can also be used for the receive section. Transmission as well as reception of a signal in a particular direction, require that the signal of each antenna element be phase and amplitude weighted similarly. For transmission, the weights are applied on the emitted signal while during reception, it is the phase and amplitude of the received signal which must be weighted for coherent addition of the signals from every element.

For 4.19 shows an antenna element used only for transmission. An optical signal is sent to every element via a fiber optic network. As described in the previous sub-sections, that signal carries the frequency, phase and amplitude information about the RF signal to transmit. The optical signal is detected and converted to RF. A power amplifier is used to boost the signal level before transmission.

Fig. 4.20 shows a receive only implementation of an element. The received signal is mixed with a local oscillator signal containing the same phase and amplitude information as a signal which would be transmitted in the direction of interest. By properly phase and amplitude weighting the LO signal from each elements with the techniques proposed before, the IF signal from each elements would then all be in phase. The IF signals may consequently be added coherently and redirected to the central processor.

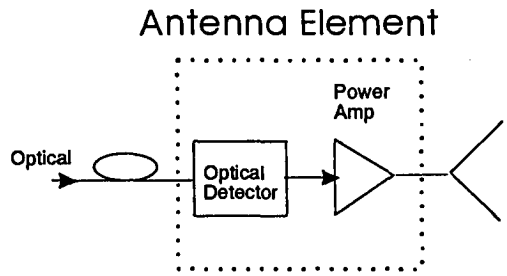

Figure 4.19 Antenna element for transmit mode only.

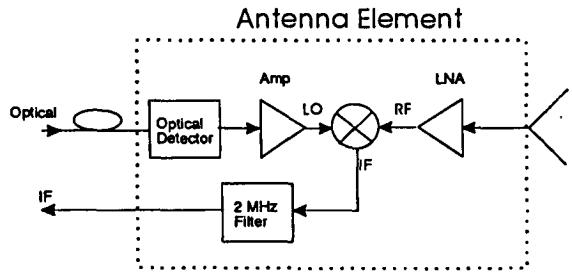

Figure 4.20 Antenna element for receive mode only.

In the case of radar applications, where the transmit and receive signals are time shared, those two functions can be grouped on the same element as shown in Fig. 4.21. During transmission, the RF signal is directed to the radiating element of the antenna. During reception, this same signal is used as the local oscillator to the mixer. Two RF switches are used to properly direct the signals. The resulting IF signal is amplified and carried to the central processor.

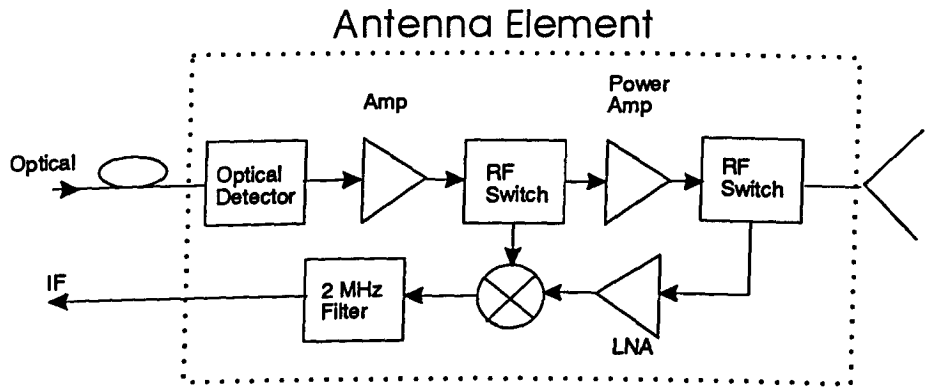

Figure 4.21 Antenna element for both transmit and receive operations.

5.0 DISTRIBUTION NETWORK

Fig. 5.1 shows a typical implementation of a fiber optic network for array antenna. The distribution network performs four different functions:

a. coupling of the optical signal into fiber optics,
b. splitting and routing the signal to reach every antenna element,
c. propagation,
d. emitted out of each fiber for detection at the antenna elements.

The first two functions may be done in reverse order or simultaneously according to the system design, as will be seen later in this chapter.

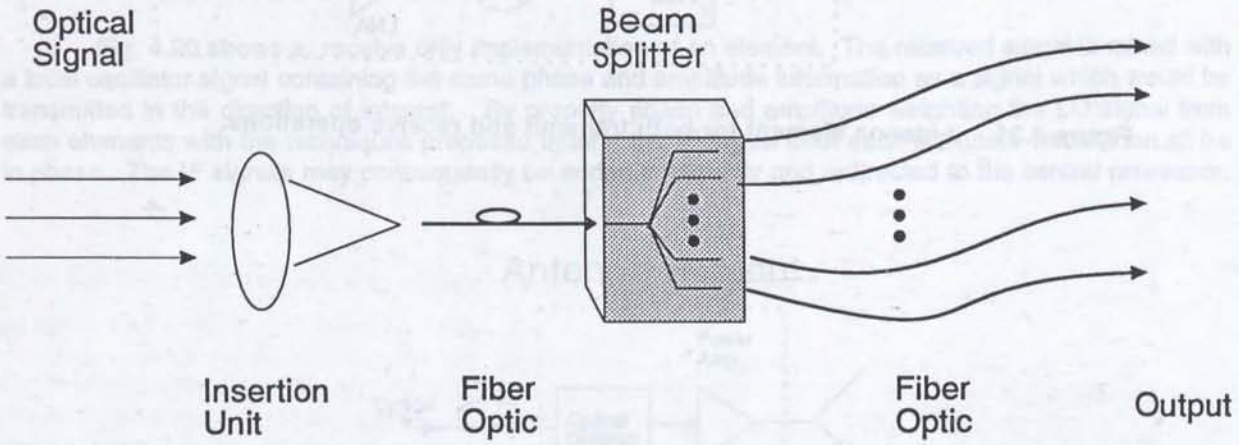

Figure 5.1 Typical distribution network for an MBA or PA antenna

Each function must be carefully examined to maximize the performance of the network, to minimize the insertion and propagation losses, to maximize the bandwidth of information-carrying capacity, to reduce the number of components. In this chapter each of the four functions are analyzed with the perspective of maximizing the performance. Different implementation strategies are reviewed and a performance analysis is done.

5.1 Source coupling

Due to the extremely small size of the propagating region, called the core (4 to 8 μm for single mode fiber and 50 to 200 μm for multi-mode), energy coupling in the fiber must be done very carefully. Their exists a number of coupling techniques differing in their complexity, coupling efficiency and cost.

5.1.1 Butt coupling

This approach is certainly the simplest, but also the least efficient. It involves only the fiber optics and the optical source, no focusing units. Consequently, if the optical beam is larger than the fiber core (4-8μm or 50-200 μm) their will be losses. Typical coupling efficiency for butt coupling is in the order of only a few percent.

5.1.2 Lens assembly

A lens assembly to focus the light beam into the fiber end will increase considerably the coupling efficiency. The efficiency will depend mainly on the lens assembly used. An important factor to consider in this case is the numerical aperture (NA) of both the lens and the fiber. The NA defines the maximum acceptance angle of light incoming on the lens or the fiber end and is defined by:

$$NA = \sin\theta = (n_1^2 - n_2^2)^{1/2}$$

where θ is the half cone angle of acceptance and n_1, n_2 are the refractive index of the core and cladding of the fiber respectively.

The numerical aperture of the lens will define the amount of light which can be collected by the light. If the incoming light is close to being collimated, the NA of the lens has very little impact. However, if one wants to focus light emerging from a laser diode into a fiber, than the lens NA aperture becomes an important issue. The emission pattern of a typical laser diode has a divergence angle of approximately 30° in one plane and 10° in the perpendicular plane. To collect all the light emerging from the diode, the NA of a lens must be at least equal to 0.5.

A typical single mode fiber, as a numerical aperture of 0.13 which corresponds to a half-cone angle of acceptance of 7.5° whereas a typical multi-mode fiber with a core of 50μm has a half-cone acceptance angle of 11° (NA=0.20) and 16° for a 62.5μm core (NA=0.275). However, by means of suitable combinations of the core and cladding, acceptance angles between 30 and 100 degrees can be obtained with glass and plastic fibres. Doped silica fibres have a more restricted acceptance angle of typically 25 degrees (NA=0.4).

The following gives a number of lens assembly which are commonly used.

5.1.2.1 Spherical lens. This type of lens is very common in bulk free space optics. With the advent of laser diodes, compact housings have been designed and are readily available. Typical NA ranges from 0.2 to 0.6 with clear aperture in the order of 5 mm. Note that since the output beam of a laser diode has different diverging angles in parallel and perpendicular plane to the emitting region, spherical lens will not be able to focus the light beam into a single spot. Typical coupling efficiency with spherical lens may reach 30% in single mode fiber up to 50% in multi-mode fiber.

5.1.2.2 Aspheric lens. Aspherical lens, with different focal lengths for each plane should be used to improve the coupling efficiency. The coupling efficiency is greatly increased and may reach up to 90%. The cost of aspheric lenses is much higher than spherical lenses.

5.1.2.3 GRIN lens. The use of GRIN (graded index) lens may allow a significant reduction in size of the lens assembly when compared to spherical and aspherical lenses. GRIN lens have the same focusing properties as the spherical lenses but instead of operating on the physical dimension of the lens, it is the variation of the refractive index which make the focusing to take place. Typical coupling efficiency in single mode fiber with GRIN lens may reach 30% while for multi-mode it may go up to 50%.

5.1.2.4 Fiber Optics. By some etching or fusion process, the tip of the fiber optics may be given the form of a spherical lens. This way, a lens assembly is not needed and the coupling unit may be made smaller. This technique is however very complex and requires special equipment to form the fiber tip.

5.2 Splitting / Routing

The second function of the distribution network, is to split and route the optical signal in order to illuminate each element of the antenna. Splitting may be divided into two main categories - free space or guided optics.

5.2.1 Free Space

In this case, the splitting / routing is done in free space, rather than in fiber optics or integrated waveguides. A number of techniques may be used depending on the applications. Beam splitters and microlens arrays are used for splitting whereas gratings, acousto-optics deflectors and deformable mirrors are mainly used for routing.

5.2.1.1 Beam splitter. The most common free space power splitting unit is certainly the conventional "beam splitter" which divides the optical power into two paths according to the reflection coatings on the glass surface. The power ratio between the two paths can take almost any values. Typical insertion losses are in the order of 0.03 dB to 1 dB.

5.2.1.2 Micro-lens array. An array of micro-lens may also be used to split an incoming beam into small sections, each being collected by a fiber optics for distribution to a different part of the antenna. Microlens array can be fabricated by holographic techniques but the most popular approaches is by micromaching or etching. Insertion loss for microlens array will mainly depend on how much light can be collected by the different elements.

5.2.1.3 Gratings. Diffraction gratings are optical elements whose surface are modulated with a highly regular groove or slit pattern. The most efficient gratings are when the grooves have a rectangular shape. The angle of the hypotenuse is called the blazing angle. The elements can be either transmitting or reflecting. The efficiency of the grating, or the fraction of light that ends up being diffracted is a function of the optical wavelength (λ), the groove spacings (d), the blazing angle of the grooves (θ_B) and the angle of incidence (θ_i). With incident light perpendicular to the grating, the efficiency peak is always exactly where $\lambda/d = 2\sin\theta_B$ and approaches 100%. Multiple blazing angles will result in various diffraction angles for various wavelength. This technique may then be used for wavelength multiplexing / demultiplexing. Gratings are usually constructed by micromachining or by holographic techniques. Gratings are consequently used more for routing than for splitting

5.2.1.4 Acousto-optics. Acousto-optics (A-O) splitting is similar to the grating. In this case the grating is done by an acoustic wave propagating inside a crystal. The acoustic wave is generated by a piezo-electric crystal excited by an RF signal. Multiple output angles are possible if multiple RF frequencies are used as the excitation source. Intensity control in each output branch is also possible by varying the intensity of the RF signal. The diffraction efficiency of A-O cells are somewhat low, in the order of 20 to 50%, which gives insertion losses around 3 to 7 dB.

5.2.1.5 Deformable mirror. A deformable mirror, as described in section 4.2.2.2, may also be used to split and direct an optical beam into may components. In this case, the individual mirrors would be mounted on tilting hinges to direct the incident light in specific locations. The incoming beam on the deformable mirror would then be split by the many small mirrors and each part be directed according to the position of the individual mirrors.

5.2.2 Guided Optics

Guided optics units may also be used for splitting and routing of the signal. These units may be divided into either passive or active components.

5.2.2.1 Passive splitters In these units, the input light signal is split in a ratio defined during the fabrication of the unit. Distribution index lens [5.1], planar waveguide branches[5.2], fused fibres [5.3] and waveguide star coupler [5.4] are a few of the passive splitter being used.

5.2.2.2 Active splitters Active splitters are usually based on the waveguide branch structure with the addition of electrodes to control the amount of light being coupled in each branch. Coupling is done by evanescent fields transferring from one fiber to the other. The electrodes changes the refractive index of the waveguide which results in different coupling ratio. Directional couplers have insertion losses between 0.1 to 0.75 dB.

5.3 Propagation

Once the signal is in the fiber and propagates, it may also experience some losses due to fiber attenuation, and connector or splice losses if a number of fibres have to be connected together. Optical amplifiers are also available.

5.3.1 Attenuation

Attenuation in fiber optics is mainly due to absorbtion and scattering. As seen in Table 2.1, absorbtion losses are lower in the 1.3 - 1.5 μm range with 0.01 dB/km loss. In the 0.8 μm region the losses increase to 2 dB/km.

5.3.2 Connector loss

Connector losses are due to misalignment between the core of one fiber to the next. Typical optical losses due to the connectors range between 0.7 to 1.0 dB.

5.3.3 Splice loss

If the fibres are joined together permanently using fusion, welding or chemical bonding, the loss introduced may be lowered to about 0.2 dB.

5.3.4 Optical amplification

There are two types of optical amplifiers.

5.3.4.1 Fiber amplifier These amplifiers operates on the principle that by pumping light into a rare-earth doped optical fiber, at a specific wavelength, that light will be converted and used to amplify the desired signal (Fig. 5.2 a). There are basically three types of fiber amplifiers classified according to the doping material included in the fiber: Erbium, Neodymium and Praseodymium. Only the Erbium doped amplifier is commercially available. These amplifiers operate only at specific frequencies. The Erbium amplifier operates at 1550 nm while the other two are for 1300nm.

5.3.4.2 Semi-conductor optical amplifier (SOA) A schematic diagram of a SOA is depicted in Fig. 5.2 b). A semi-conductor laser, which is anti-reflection coated to prevent lasing, is inserted between two fibres to provide amplification. Gain is obtained by electrical pumping. Compared to the fiber amplifiers, SOA are smaller in size, consume less power, are compatible with integration and are expected to be low cost to produce. However, the gain obtained is smaller than with fiber amplifiers. Moreover, SOA are polarization sensitive, have wavelength gain ripple, are difficult to produce with low noise figure and low coupling loss [5.5]. Unlike the fiber amplifiers, the SOAs will operate at any wavelength, as long as the amplifier and the optical signal to be amplified are at the same wavelength.

Table 5.1 gives a comparison of the two types.

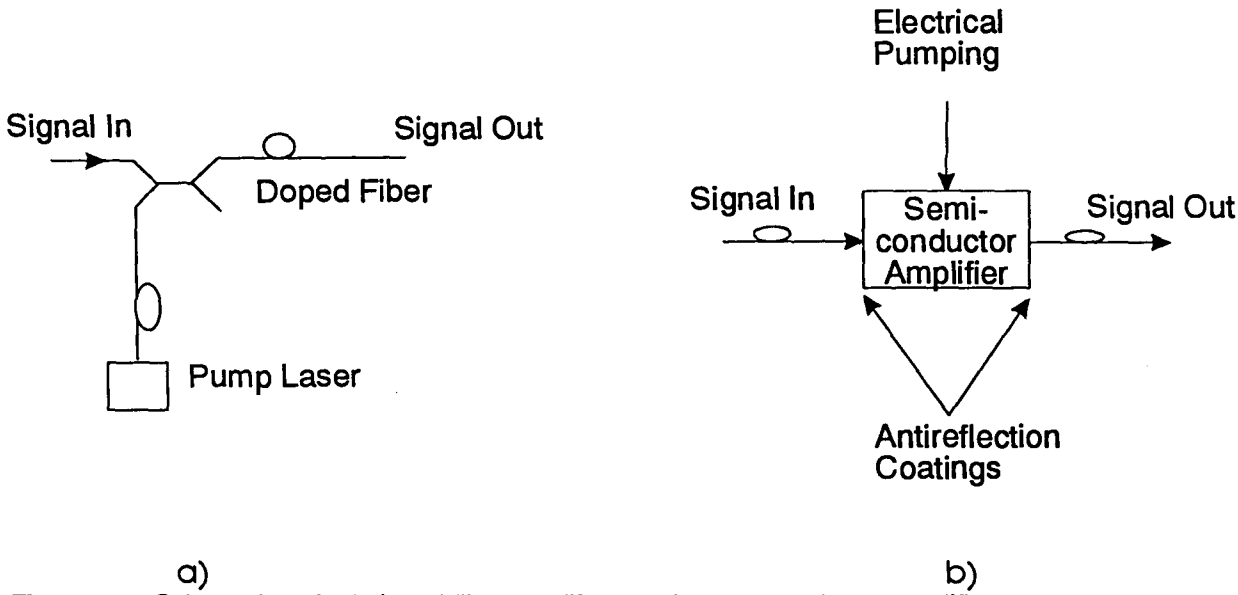

Figure 5.2 Schematics of a) doped-fiber amplifier and b) semi-conductor amplifier.

Table 5.1 Comparison of two commercially available optical amplifiers.[Ref. 5.6]

	Erbium Doped	Semi-conductor
Net Gain	35 dB	20 dB
Output power	+15 dBm	+3 dBm
Bandwidth	45 nm	45 nm
Centre Wavelength	1550 nm	780-900, 1300, 1550
Pump	980 nm or 1480 nm	Electrical
Time Constant	1 ms	1 ns
Polarization sensitivity	0.5 dB	1.0 dB
Noise Figure	3-4 dB	8-10 dB
Status	Commercially Available	Commercially Available

5.4 Link budget

In this section, the link budget of a very simple architecture will be elaborated. The architecture is shown in Fig. 5.3. Only the transmit section will be done here. A thousand elements must be driven and direct modulation of laser diodes is assumed. The distribution network only carries the frequency reference; phase and amplitude controls are done on the RF signal after detection at each antenna element. Table 5.2 describes the link budget. The entries in the table have been covered in the various sections of this report and are summarized in Table 5.3.

Table 5.2 indicates that to drive the 1000 antenna elements, ten lasers directly modulated lasers would be required, with an RF signal generator power of 174 mW. Each optical signal would be split in five branches. A 30 dB amplification of the RF signal, at each of the 50 detectors, and a further 35 dB of amplification at each element is also necessary. A system margin of 3 dB has been assume. It must be noted that the splitting ratios can be modified to optimize the architecture in terms of either the number of lasers, the power amplifications at each element, the total power consumption...

It must also be noted that since photodetectors are current devices, any split of the optical signal will result in detected RF power losses equal to the square of the splitting ratio. For example, in Table 5.3, the optical signal is split in five branches, consequently, the associated RF power into a 50 ohm load will be 25 times lower than a system with no optical split. That is to say that in order to minimize the RF amplification at the antenna elements, the signal splitting should be done at the RF level rather than at the optical level.

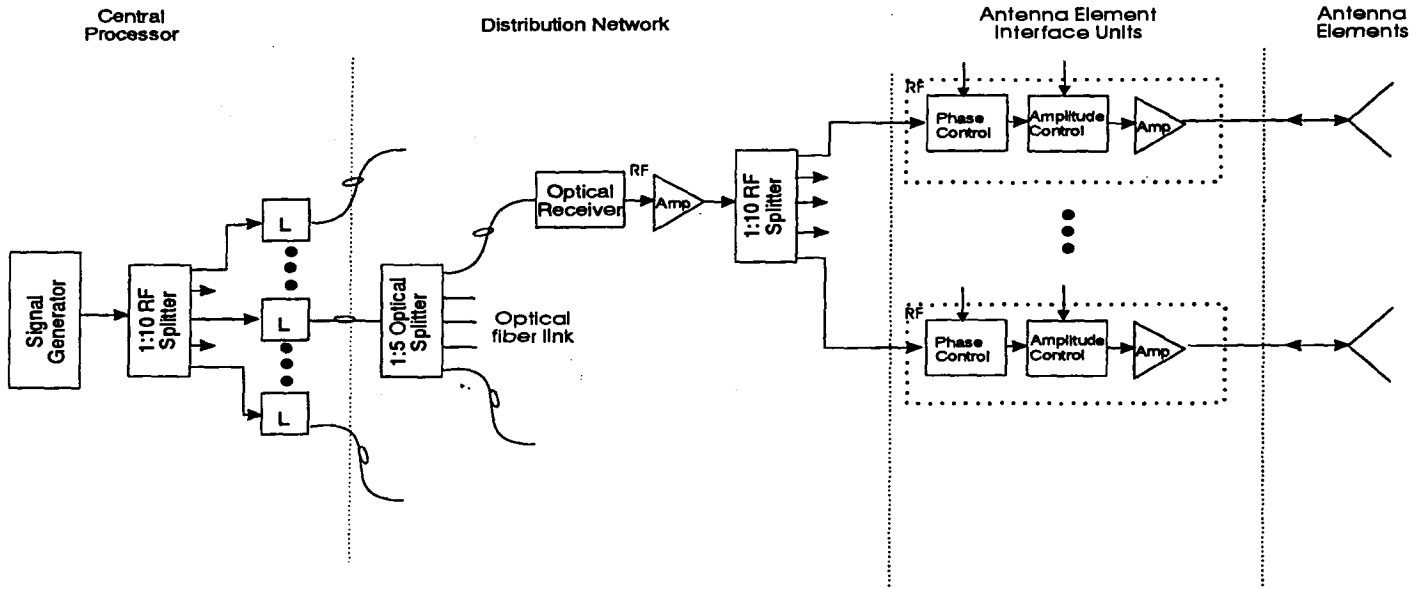

Figure 5.3 Possible architecture for the transmit section of a 1000 element antenna.

Table 5.2 RF / Optical link budget for the architecture shown in Fig. 5.3

Central Processor					
	Signal Generator power (mw)				173.61
	RF splitting ratio (1:N)		10		
	RF splitting loss (dB)	-10.00			
	RF power per laser (mW)				17.36
	Current per laser (assumed to be a 10 ohm load), mA		41.67		
	RF-to-Optics conversion efficiency (mW/mA)	0.60			
	Maximum laser power (mW)				50
	Modulation depth (%)		50		
	Average optical power (mW)				25.00
	AC coupled optical power (mW)				25.00
	Number of lasers required			10	
Distribution Network (for one laser link)					
	Insertion loss in fiber	-3			
	Optical splitting ratio (1:N)		5		
	Splitting loss (dB)	-6.99			
	1:2 splitter excess loss (0.5 dB per splitter)	0			
	1:4 splitter excess loss (1.0 dB per splitter)	0			
	1:8 splitter excess loss (1.7 dB per splitter)	-3.4			
	Splice loss (dB)	-0.5			
	Fiber loss (dB)	-0.1			
	Useful optical power per optical receiver (mW)				9.98E-01
	Optical receiver conversion efficiency (mA/mW)	0.6			
	Photodetection current generated (mA)			0.60	
	Associated RF power into a 50 ohm load (mW)				0.017915
	RF power amplifier (dB)	30			
	Useful RF power (mW)				1.79E+01
	Size of a tile (sq meter)			5.70	
	RF splitting ratio (1:N)		20		
	Average RF splitting loss (dB)	-13.01			
	RF splitter excess loss (dB)	-0.20			
	Average RF propagation loss (dB) (0.5dB/m)	-0.30			
	RF power per AEIU (mW)				7.99E-01
Antenna element interface unit					
	Phase shifter loss (dB)	-0.1			
	Attenuator excess loss (dB)	0			
	Power amplification (dB)	34.58			
	Circulator loss (dB)	-0.5			
System margin (dB)		-3			
Output RF power (mW)					1000.00

Table 5.3 Typical parameters for an optical link budget.

Matching Losses	
Unmatched	frequency dependant (high)
Resistive matched	frequency dependant (high)
Lossless matched	0.1-0.5 dB
RF-to-Optics conversion	
Direct modulation	0.6 mw/mA
External modulation	0.5 to 1 W of RF with maximum output optical power of 3-5 mW
Coupling Losses	
Laser-to-fiber / fiber-to-detector	
Butt coupling	7-10 dB
Spherical lens	2-3 dB
GRIN lens	2-3 dB
Aspherical lens	0.5 dB
Optical phase shifters insertion loss ($LINbO_3$)	4 dB
Splitters excess losses	
1:2	0.5 dB
1:4	1.0 dB
1:8	1.7 dB
Fiber propagation losses	
830 nm	2 dB/km
1330 nm	0.02 dB/km
1550 nm	0.01 dB/km
Optics-to-RF conversion efficiency	0.6 mA/mW

6.0 CONCLUSION

This report has done a survey of the optical technology for application in phased-array and MBA antennas. Optical techniques, for calculating and applying the phase and amplitude weights necessary to beam forming networks have been discussed. Conversion of the RF signal to the optical domain and back have also been addressed. Finally, fiber optic distribution network was reviewed including a link budget example.

Amongst the main system architectures discussed, it is difficult to select the best one. They widely differ in terms of their technological maturity as well as in terms of their processing capability. Each application will require a detailed system study to identify the best suited architecture for its own special requirements. If one was to divide the system architectures presented in terms of their technological maturity, the following division would probably pertain.

Long term architecture (over 10 years): The architecture which offers the best potential in terms of processing capability is unfortunately the least mature one. With Fourier optic technology, there is no need to digitally compute the phase and amplitude weights needed for beam steering, nor to use phase shifters and attenuators, the optical system performs all these functions automatically, in real time. However, the main component of the system, the one which transfer the image of the beam shape into phase and amplitude information, the spatial light modulator, requires a lot of development. High contrast (10,000 : 1) two-dimension spatial light modulators will be needed before this technique can be used. High power lasers and efficient coupling efficiency will be required since processing of every antenna element must be done by the same system.

Mid-term architectures (5 to 10 years): The architectures involving deformable mirror and time delay units seem to be more in-line for a mid-term realisation. The former would serve in systems where small signal bandwidths are involved while the latter would be needed when beam scanning due to large bandwidth causes a problem. These architectures allow, as with the Fourier optic architecture, phase and amplitude weigthing remotedly from the antenna, in the payload. In these architectures however, computation of the weigths must be done digitally. Improvement of the deformable mirror and the time delay units is however needed. Extremely high resolution in the deformation of the mirror (steps of 1nm over a 1μm swing) will be needed. As for the time delay units, improvements will have to be done to lower the signal loss, to reduce the size of the units and the switching power requirements.

Short-term architecture: There are a number of architectures which could be built with today's technology, or with some improvement of existing components. The most obvious one would rely on optics exclusively for signal frequency distribution. Phase and amplitude weighting would be done at the antenna elements, on the RF signal, based on digitally computed values. If the number of differently weighted element is not to large, signal conditioning could be done in the payload on the RF signal or on the optical signal. To each RF phase shifters would be associated one laser, or one optical modulator.

A real challenge also exists in the R&D of the components. Among the components discussed throughout this report, the following activities should be pursued.

High power laser diode. High power laser diodes will be required to compensate the high splitting losses in the distribution network to hundreds of antenna elements. Splitting ratios up to 1:100 may be needed. To lower the overall power requirements, the conversion efficiency of the lasers will

need to be improved.

Generation of RF signal using optical heterodyne methods. The aim of this research would to develop a prototype model of an RF signal generator using a 2 or 3 laser heterodyne configuration, as shown in section 2.3, to generate the required RF signal. Research for improving the efficiency (optical losses and RF-to-optics conversion) of integrated optics phase modulators, as described in section 2.2.2.2, is also needed. These units could generate a wide range of RF frequencies without the need of large RF devices.

Micro-lens matrix. For free space BFN architectures (Fourier optics, deformable mirrors), a matrix of micro-lens will be required to efficiently focus the light beam into the many fiber optics. This micro-lens could be fabricated using a number of techniques, namely holography, gratings, Fresnel zone plates...

Deformable mirror. One promising architecture proposed used deformable mirror to apply the phase weigthings. Development of such mirrors is already underway but more R&D is needed to meet the stringent requirements. Phase settings should be accurate to less than 0.2°, which means displacement resolution of the mirror of less than 1 nm. Response time in the order of a few microseconds would also be needed. Moreover, the mirror should modify only the phase front and not the amplitude. The mirror should be approximately one square inch and be able to control over 16,000 antenna elements.

Optics-to-RF conversion. This research is required to increase the conversion efficiency between the optical signal and the RF domain at the antenna element, in order to lower the power requirements.

Time delay units. Research should be pursued for the fabrication of time delay units. Effort should be made to reduce the size of the units, lower the signal loss and also lower the power consumption of the switches.

Optical amplifiers. To compensate for the optical losses due to signal splitting or optical modulators, amplifiers will be needed. Research should be pursued in the area of optical amplifiers, both in the doped fiber and semiconductor amplifier, to obtain minimum induced noise.

REFERENCES

Chapter 2

2.1. K. Lau, N. Bar-Chaim, I. Ury, A. Yariv, "Direct Amplitude Modulation of Semiconductor GaAs Lasers to X-band Frequencies, Appl.Phys.Lett. 43,p.11

2.2. R. Simons "Optical Control of Microwave Devices", R. Simons, Artech House, 1990, p.37.

2.3. Ortel Corporation laser module model 1515B. As of January 1991, the 12GHz 0.8μm GaAlAs laser diode line is discontinued.

2.4. K. Uomi, T. Mishima, N. Chinone, "Ultrahigh Relaxation Oscillation Frequency (up to 30 GHz) of Highly Doped GaAs/GaAlAs Multiple Quantum Well Lasers," Applied Physics Letters, Vol.51, No.2, July 1987, pp. 78-80.

2.5. Ortel Corp. 1.3 μm InGaAsP diode

2.6. B.C. Lam, A.L. Kellner. F.K.L. Yu, "High Speed Fiber Optic Link by External Modulation of Mode Locked Laser", SPIE vol. 1703, April 1992, pp.541-544.

2.7. S. Kobayashi, Y. Yamamoto, M. Ito, T. Kimura, "Direct Frequency Modulation in AlGaAs Semiconductor Lasers", IEEE JQE, vol. QE-18, No.4, April 1982, pp. 582-595.

2.8. N.J. Berg, J.N. Lee, "Acousto-Optic Signal Processing Theory and Implementation", Dekker, New-York, 1983.

2.9. T. Higgins, "There is a Lot More to an A-O Modulator Than Meets The Eye", Laser Focus World, pp. 133-143, July 1991.

2.10. R. Simons, "Optical Control of Microwave Devices", Artech House, 1990, p.62

2.11. Alferness, "Waveguide Electrooptic Modulator", IEEE Trans. MTT, vol30, no8, 1982, pp.1121-1137

2.12. T. Sueta, M. Izutsu, "Integrated Optic Devices for Microwave Applications", IEEE Trans on Microwave Theory and Techniques, vol. 38, No. 5, May 1990, p. 477-482.

2.13. T. Sueta, M. Izutsu, "High Speed Guided-Wave Optical Modulators", Japan Annual Reviews in Electro-optic Computing and Telecommunications, Optical Devices and Fibers, pp. 140-150

2.14 H. Taub, D.L. Schilling, "Principle of Communication Systems", McGraw-Hill, 1971, pp.114-120.

2.15 B. Culshaw, M.G.F. Wilson, "Integrated optics frequency shifter modulator", Electronics Letters 5 Feb 1981, vol. 17, no. 2, pp.135-136

2.16 M. Izutsu, S. Shikama, T. Sueta, "Integrated optical SSB modulator / frequency shifter", IEEE Journal of quantum electronics, Vol. QE-17, no. 11, november 1981, pp.2225-2227.

2.17. B.E.A. Saleh, M.C. Teich, "Fundamentals of Photonics", Wiley Series in Pure and Applied Optics", J.W. Goodman Ed., 1991, chap 7 section 4. p.266

2.18. B.E.A. Saleh, M.C. Teich, "Fundamentals of Photonics", Wiley Series in Pure and Applied Optics", J.W. Goodman Ed., 1991, chap 7 section 4. p.267.

2.19. R. Simons, "Optical Control of Microwave Devices", Artech House, 1990, p.62

2.20. K. Wakita, I. Kotaka, O. Mitomi, H. Asai, Y. Kawamura, M. Naganuma, "High-Speed InGaAlAs/InAlAs Multiple Quantum Well Optical Modulators", IEEE Journal of Lightwave Techn., vol.8, no.7, Julay 1990, pp. 1027-1031.

2.21. R.G. Walker, "High-Speed III-V Semiconductor Intensity Modulators", IEEE Journal of Quantum Electronics, vol.27, no.3, March 1991, pp.654-667.

2.22. R.G. Walker, A.C. Carter, " Electro-optic modulators in III-V materials for microwave bandwidths", Proc. SPIE, vol. 995, Sept 1988, pp.27-30.

2.23. S.K. Korotky, G. Eisentstein, R.S. Tucker, J.J. Veselka, G.Raybon, "Optical Intensity Modulation to 40 GHz Using a Waveguide Electro-Optic Switch", Applied Physics Letters, vol. 50, no. 23, 8 June 1987 pp.1631-1633.

2.24. P.S. Cross, A. R.A. Baumgartner, B.H. Kolner, "Microwave Integrated Optical Modulator", Applied Physics Letters, vol. 44, no 5, 1 March 1984, pp. 486-488.

2.25. C.M. Gee, G.D. Thurmond, H.W. Yen, "17-GHz Bandwidth Electro-Optic Modulator", Applied Physics Letters, vol. 43, no. 11, 11 Dec. 1983, pp.998-1000.

2.26. L. Goldberg, A.M. Yurek, H.F. Taylor, J.F. Weller, "35 GHz Microwave Signal Genearation With an Injection-Locked Laser Diode", Electronics Letters, Vol. 21, No. 18, August 1985, pp.814-815.

Chapter 3

3.1 G. Keiser, "Optical Fiber Communications", New-York, Mc-Graw-Hill, 1983, chap. 6. To be verified.

3.2 New Focus, model 1404.

3.3 D. Wake, T.P. Spooner, S.D. Perrin, I.D. Henning, "50 GHz InGaAs Edge-coupled pin photodetector", Electronics Lett., vol.27, no.12, 6 June 1991, pp. 1073-1075.

3.4 R.S. Tucker, A.J. Taylor, C.A. Burrus, G. Eisentein, J.M. Weisenfeld, "Coaxially mounted 67 GHz bandwidth InGaAs PIN photodiode", Electronics Lett., vol. 22, 1986, pp.917-918.

3.5 D.G. Parker, "Use of transparent Indium Tin Oxide to form a highly efficient 20 GHz Schottky-barrier photodiode", Electronics Letters, Vol. 21, No. 18, Aug. 1985, p.778

3.6 H. Blauvelt, G. Thurmond, J. PArsons, D. Lewis, H. Yen, "Fabrication and characterization of GaAs Schottky barrier photodetectors for microwave fiber optic links", Appl. Phys. Lett., vol 45, no 3, 1

Aug. 1984, pp. 195-196.

3.7 New Focus Inc. Mountain View, California, model 1002

3.8 S.Y. Wang and D.M. Bloom, "100 GHz bandwidth planar GaAs Schottky photodiode", Electronics Letters, vol. 19, no. 14, July 1983, pp.554-555.

3.9 D.G. Parker, P.G. Say, A.M.m Hansom, "110 GHz High-efficiency photodiodes fabricated from indium tin oxide / GaAs", Elect. Letters, 7 May 1987, vol.23, no. 10. pp. 527-528.

3.10 J. Selders, N. Emeis, H. Beneking, "Schottky-barriers on p-type GaInAs", IEEE Trans. on Electron Devices, Vol. ED-32, no. 3 March 1985, pp.605-609.

3.11 N. Emeis, H. Schumacher, H. Benenking,"High Speed GaInAs Schottky photodetector", Electronics Lett., vol 21, no. 5, 28 Feb. 1985,pp.180-181.

3.12 D. Atkinson, C. Dreze, A. Waksberg, "Technology development for wideband intersatellite laser communication systems", MPB Technology Inc, DSS contract no. 36001-7-3591/01-ST, 27 June 1990, p.4-38, Fig. 4-20 a).

3.13 R. Simons, "Optical control of microwave devices", Artech House, 1990, p.106.

3.14 K.L. Tan et als, "60 GHz Pseudomorphic $Al_{0.25}Ga_{0.75}As/In_{0.28}Ga_{0.72}As$ low noise HEMT's", IEEE Electron Device Letters, vol.12, no.1, Jan 91, pp.23-25.

3.15 K.L. Tan et als, "94-GHz 0.1μm T-gate low-noise pseudomorphic InGaAs HEMT's", IEEE Electron Device Letters, vol.11, no.12, Dec 90, pp.585-587.

3.16 R. N. Simons, "Microwave performance of an optically controlled AlGaAs/GaAs high electron mobility transistor and GaAs MESFET", IEEE Trans. on microwave theory and techniques, Vol. MTT-35, no. 12, Dec. 87, pp. 1444-1455.

3.17 K. Kurokawa, "Injection Locking of Microwave solid-state oscillators", Proceedings of the IEEE, vol 61, no.10, Oct. 73, pp. 1386-1410.

3.18 A.A.A. DeSalles, "Optical Control of GaAs MESFET's", IEEE Trans on microwave theory and techniques, vol. MTT-31, no 10, Oct. 83, pp.812-820.

3.19 A. Seeds, A.A.A. DeSalles, "Optical control of microwave semiconductor devices", IEEE Trans on microwave theory and techniques, vol. MTT-38, no 5, May 90, pp.577-584.

3.20 C. Beaulieu, "Synchronisation d'oscillateurs micro-ondes par injection optique directe", Thèse de maîtrise, Université Laval, Septembre 1993.

Chapter 4

4.1. A. Daryoush, P. Herczfeld, V. Contarino, A. Rosen, Z. Tursk, and P. Wahi, "Optical Beam Control of mm-Wave Pahsed Array Antennas For Communications", Microwave Joumal, March, pp.97-104, 1987.

4.2. R.L. Johnson, "Opto-Electronic Phased Array Antennas", IEEE MilCom 1986, pp.42.3.1 - 42.3.5.

4.3. T. David, H.C. Burstyn, "Optical combinatorial logic elements for an adaptive optical processor", Proc. SPIE, vol 886, p.102, 1988.

4.4. P.R. Beaudet, J.C. Bradley, E.C. Malarkey, "Optical adaptive beamforming using residue number systems (RNSs) and Gauss elimination", Proc. SPIE, vol 886, p.112 , 1988.

4.5. E.J. Baranoski, D.P. Casasent, "Optical processing of covariance matrices for adaptive processors", Proc. SPIE, vol 886, p.140, 1988.

4.6. R.M. Montgomery, J.W. Watkins, "2-D phased-array processing in bulk wave acoustic media", Proc. SPIE, vol 886, p.189, 1988.

4.7. L.P. Anderson, F. Boldissar, D.C.D. Chang, "Antenna beamforming using optical processing", Proc. SPIE, vol 886, p.228, 1988.

4.8. K.A. Nickerson, P.E. Jessop, S. Haykin, "Optical processor for array antenna beam shaping and steering", Proc. SPIE, vol 1217, p.184, 1990.

4.9. N.A. Riza, "Acousto-optic architectures for multidimensional phased-array antenna processing", Proc. SPIE, vol 1476, p.144, 1991.

4.10. E. Toughlian, H. Zmuda, "A photonic variable RF delay line for phased array antennas", J. Lightwave Technol. vol. LT-8, no 12, pp.1824-1828, Dec. 1990.

4.11. N.A. Riza, "Transmit/receive time-delay beam-forming optical architecture for phased-array antennas", Applied Optics, vol. 30, no. 32, pp.4594-4595, 10 Nov. 1991.

4.12. W. Ng, A.A. Walston, G.L. Tangonan, J.J. Lee, I.L. Newberg, N. Bernstein, "The first demonstration of an optically steered microwave phased array antenna using true-time-delay", J. Lightwave Technol. vol. LT-9, no 9, pp.1124-1131, 1990.

4.13. H. Zmuda, E. N. Toughlian, "Adaptive Microwave Signal Processing: A Photonic Solution", Microwave Journal, February 1992, pp. 58-71.

4.14. L.H. Gesell, T.M. Turpin, "True time delay beam forming using acosuto-optics", SPIE proc. Microwave and Phased Array Processing, vol.1703, 1992

4.15. C.T. Sullivan et als, "Switched time delay elements based on AlGaAs/GaAs optical waveguide technology at 1.32 μm for optically controlled phased array antennas", SPIE proc. Optoelectronic Signal Processing for Phased Array Antennas III, vol.1703, no.36, 1992.

4.16. J. H. Hong, "Broadband phased array beamforming", Proc. SPIE, vol 1102, pp.134-141, 1989

4.17. W. Charczenko, P. Surette, P. Matthews, H. Klotz, A.R. Mickelson, "Integrated Optical Buttler Matrix for Beam Forming in Phased Array Antennas", SPIE proc. 1217, January 1990, pp. 196-206.

4.18. W.L. Stutzman, G.A. Thiele, Antenna Theory and Design, John Wiley & Sons, New-York, 1981.

4.19. J.E. Hudson, Adaptivee Antenna Principles, Peregrinus, London, 1981

4.20. T.C. Cheston, J. Frank, Radar Handbook chapter 11, Ed. Skolnik M.I., Mc-Graw-Hill, 1970.

4.21. L. Liu, W. Jones, R. Carandang, W. Lam, J. Yonaki, D. Streit, R. Kasody, "Phased Array Receiver Development Using High Performance HEMT MMICs", SPIE proc. vol 1475, April 1991, pp.193-198.

4.22. T. Sato, H. Ishida, O. Ikeda, "Adaptive PVDF piezoelectric deformable mirror system", Applied Optics, vol. 19, no.9, 1may 1980.

4.23. C.M Schiller, et als, "Charge-Transfer-Plate Deformable Membrane Mirrors for Adaptive optics Applications", SPIE proc. vol 1543, July 1991, pp.120-127.

4.24. D.R. Pape, L.J. Hornbeck, "Characteristics of the Deformable Mirror Device For Optical Information Processing", Opt. Eng, 22, 1983, p.675

4.25. J.M. Florence et al., "A new deformable mirror spatial light modulator for phase modulation applications", Proc. of the 1988 conference on pattern recognition for advance missile systems, GACIAC Pr88-04, pp.379-386, Huntsville, Alabama, 1988.

4.26. E. Ackerman, et als, "Integrated 6-bit Photonic True-Time-Delay Unit for Lightweight 3-6 GHz Radar Beamformer", IEEE MTT-S Digest, 1992, pp. 681-684.

4.27. J. Goodman, "Introduction to Fourier Optics", McGraw Hill, 1968, p.86

4.28. G.A. Koepf, "Optical processor for phased-array antenna beam formation", Proceedings of SPIE, vol.477, p.75, 1984.

Chapter 5

5.1. K. Kobayashi, R. Ishikawa, K. Minemura and S. Sugimoto, Fibers Integr. Opt., 2, (1979), p.1.

5.2. E. Okuda, I. Tanaka, T. Yamasaki, Applied Optics, 23, 1984, p.1745.

5.3. S. Ohshima, T. Ito, K. Donuma, Y. Fujii, Electon. Lett., 20, 1984, p.976.

5.4. J. Minowa, N. Tokura K. Nosu, IEEE J. Lightwave Technology LT-3, 3, p.438

5.5 J. Auge, J. Chesnoy, P.M. Gabla, A. Weygang, "Progress in optical amplification", Microwave Journal, vol. 36, no.6, June 1993,pp.62-74.

5.6. J. Mellis, "Optical Amplifiers Make Their Move", Lasers & Optronics, Aug. 1991, pp.43-46.

DOCUMENT CONTROL DATA

(Security classification of title, body of abstract and indexing annotation must be entered when the overall document is classified)

1. ORIGINATOR (the name and address of the organization preparing the document. Organizations for whom the document was prepared, e.g. Establishment sponsoring a contractor's report, or tasking agency, are entered in section 8.)

Communications Research Centre
3701 Carling Avenue
Ottawa, Ontario

2. SECURITY CLASSIFICATION (overall security classification of the document. including special warning terms if applicable)

UNCLASSIFIED

3. TITLE (the complete document title as indicated on the title page. Its classification should be indicated by the appropriate abbreviation (S,C or U) in parentheses after the title.)

OPTO-ELECTRONIC TECHNOLOGY FOR THE OPTICAL CONTROL OF ARRAY ANTENNA (U).

4. AUTHORS (Last name, first name, middle initial)

CLAUDE BELISLE

5. DATE OF PUBLICATION (month and year of publication of document)	6a. NO. OF PAGES (total containing information. Include Annexes, Appendices, etc.)	6b. NO. OF REFS (total cited in document)
SEPTEMBER, 1993	74	80

7. DESCRIPTIVE NOTES (the category of the document, e.g. technical report, technical note or memorandum. If appropriate, enter the type of report, e.g. interim, progress, summary, annual or final. Give the inclusive dates when a specific reporting period is covered.)

CRC TECHNICAL NOTE #93003

8. SPONSORING ACTIVITY (the name of the department project office or laboratory sponsoring the research and development. Include the address.)

DEFENCE RESEARCH ESTABLISHMENT OTTAWA
OTTAWA, ONTARIO K1A 0Z4

9a. PROJECT OR GRANT NO. (if appropriate, the applicable research and development project or grant number under which the document was written. Please specify whether project or grant)	9b. CONTRACT NO. (if appropriate, the applicable number under which the document was written)

10a. ORIGINATOR'S DOCUMENT NUMBER (the official document number by which the document is identified by the originating activity. This number must be unique to this document.)	10b. OTHER DOCUMENT NOS. (Any other numbers which may be assigned this document either by the originator or by the sponsor)
CRC TECHNICAL NOTE 93-003	

11. DOCUMENT AVAILABILITY (any limitations on further dissemination of the document, other than those imposed by security classification)

(X) Unlimited distribution
( ) Distribution limited to defence departments and defence contractors; further distribution only as approved
( ) Distribution limited to defence departments and Canadian defence contractors; further distribution only as approved
( ) Distribution limited to government departments and agencies; further distribution only as approved
( ) Distribution limited to defence departments; further distribution only as approved
( ) Other (please specify):

12. DOCUMENT ANNOUNCEMENT (any limitation to the bibliographic announcement of this document. This will normally correspond to the Document Availabilty (11). However, where further distribution (beyond the audience specified in 11) is possible, a wider announcement audience may be selected.)

UNLIMITED

13. ABSTRACT (a brief and factual summary of the document. It may also appear elsewhere in the body of the document itself. It is highly desirable that the abstract of classified documents be unclassified. Each paragraph of the abstract shall begin with an indication of the security classification of the information in the paragraph (unless the document itself is unclassified) represented as (S), (C), or (U). It is not necessary to include here abstracts in both offical languages unless the text is bilingual).

ABSTRACT

In this report, concepts, components, performance analysis, system designs for an opto-electronic implementation of phased array and multiple beam antennas are reviewed. The aim of the report is to provide the reader with a basic understanding of what needs to be accomplished and an overview of the state of the art in opto-electronics components and systems.

RÉSUMÉ

Dans ce rapport, différents concepts, composantes, analyses de performance, et architectures de systèmes pour la fabrication d'une antenne à ouverture de phase contrôlée opto-électroniquement sont revus. Le but du rapport est d'offrir au lecteur une compréhension sommaire de ce qui doit être accompli ainsi qu'un aperçu de l'état de la technologie au niveau des composantes électro-optiques et des systèmes.

14. KEYWORDS, DESCRIPTORS or IDENTIFIERS (technically meaningful terms or short phrases that characterize a document and could be helpful in cataloguing the document. They should be selected so that no security classification is required. Identifiers, such as equipment model designation, trade name, military project code name, geographic location may also be included. If possible keywords should be selected from a published thesaurus. e.g. Thesaurus of Engineering and Scientific Terms (TEST) and that thesaurus-identified. If it is not possible to select indexing terms which are Unclassified, the classification of each should be indicated as with the title.)

- OPTICS
- OPTICAL
- OPTO-ELECTRONICS
- PHASED ARRAY
- MULTIPLE BEAM ANTENNA
- PHASED ARRAY ANTENNA
- LASER